

# Overview of two-photon and two-boson exchange

Peter Blunden<sup>†</sup>

University of Manitoba

Electroweak Box Workshop, September 28, 2017

<sup>†</sup>in collaboration with Wally Melnitchouk and AJM Collaboration

# Outline

- Recent advances in TPE theory (2008-present)

Review: Afanasev, PGB, Hassell, Raue, Prog. Nucl. Part. Phys. (2017)

- improved hadronic model parameters (fit to data)
- use of dispersion relations and connection to data
- new experimental results

- $\gamma Z$  box contributions to PV electron scattering

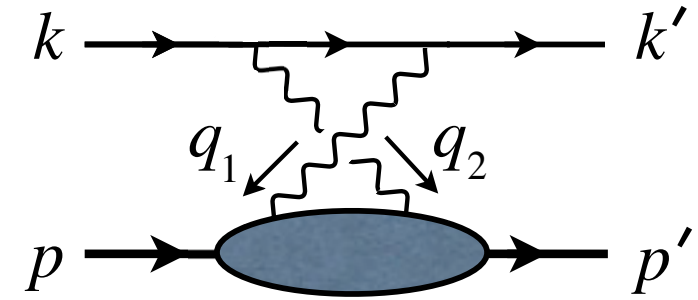
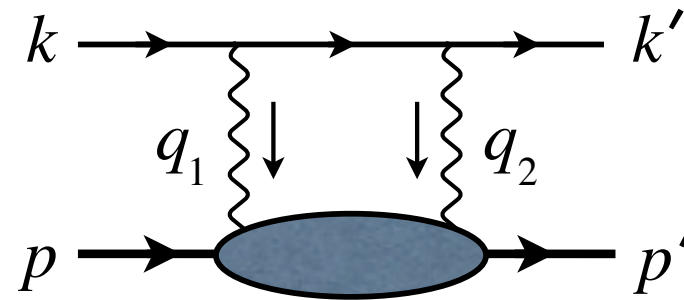
- amenable to dispersion analysis in forward limit ( $Q^2 \rightarrow 0$ )
- distinction between axial and vector hadron coupling
- use of inelastic PV data in resonance and DIS regions

# Hadronic Approach

Low to moderate  $Q^2$ :

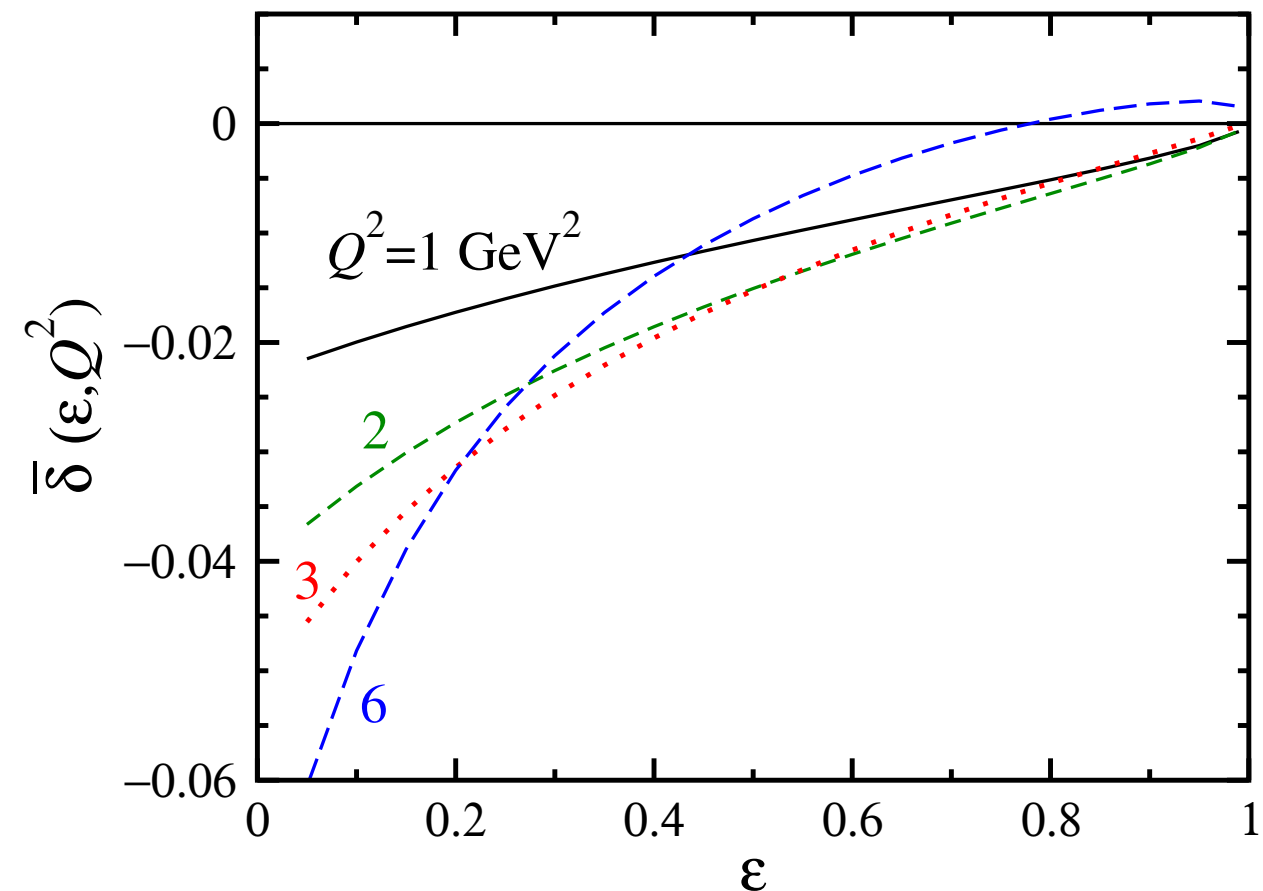
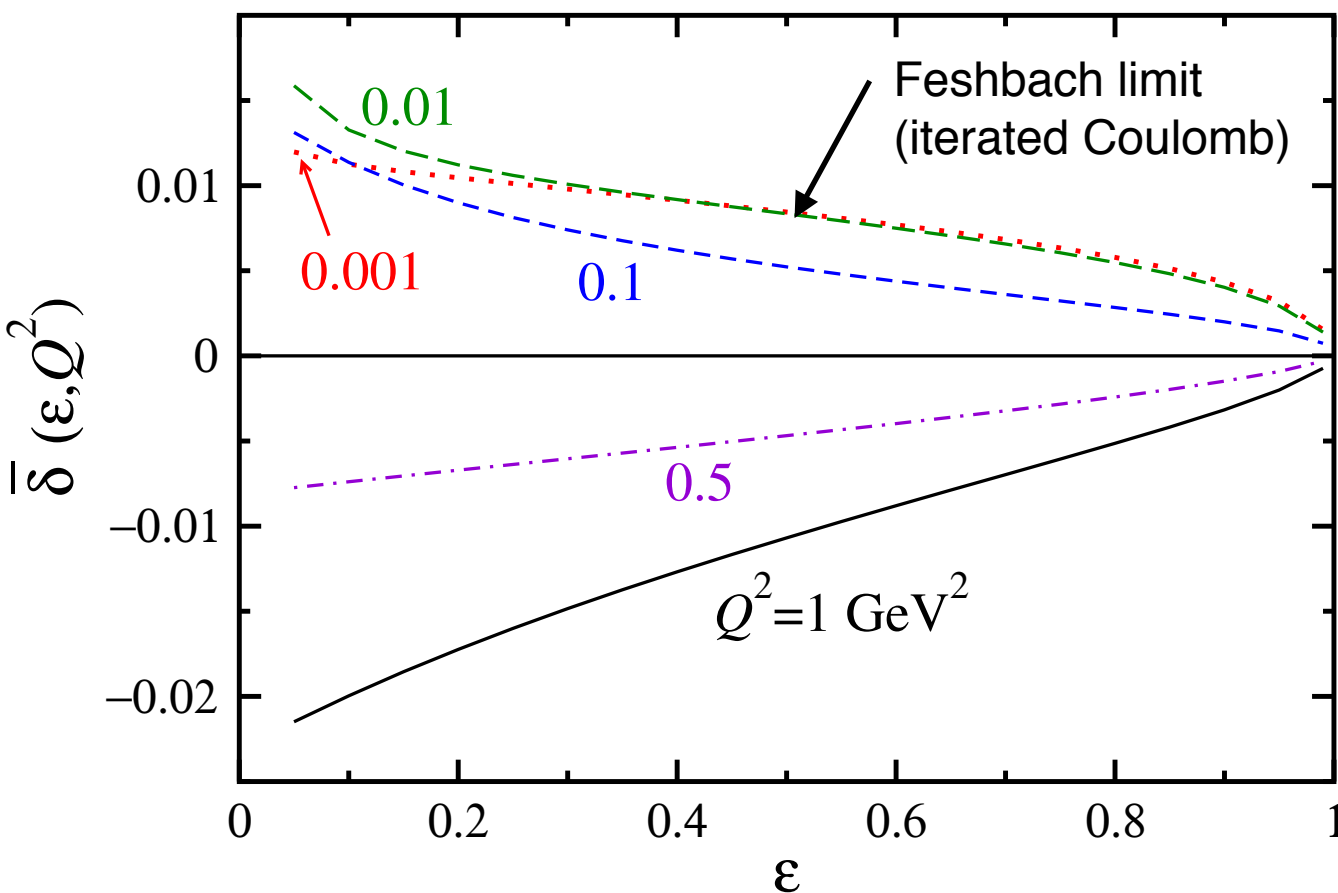
hadronic:  $N + \Delta + N^*$  etc.

- as  $Q^2$  increases more and more parameters
- Loop integration using sum of monopole transition form factors fit to spacelike  $Q^2$

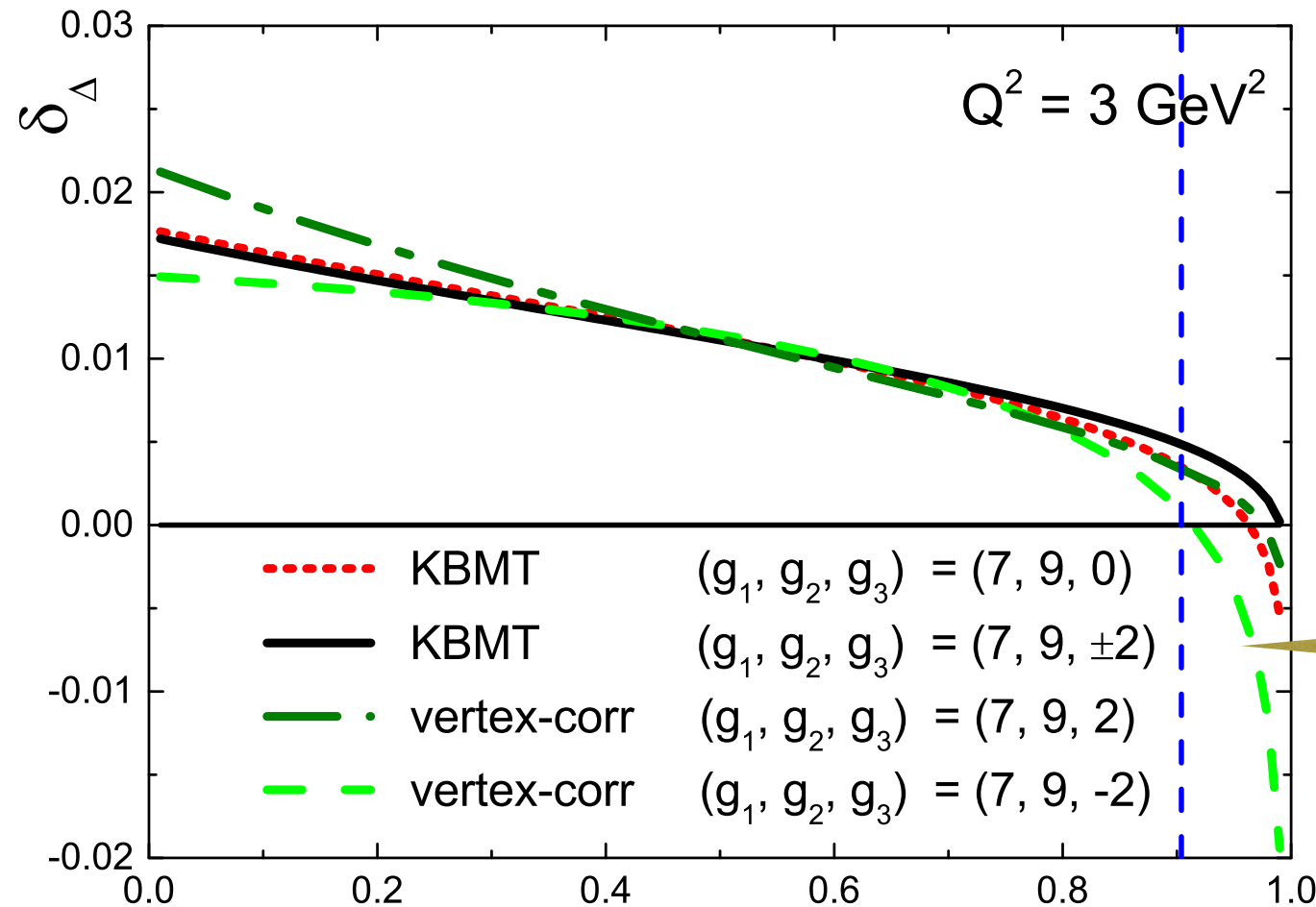
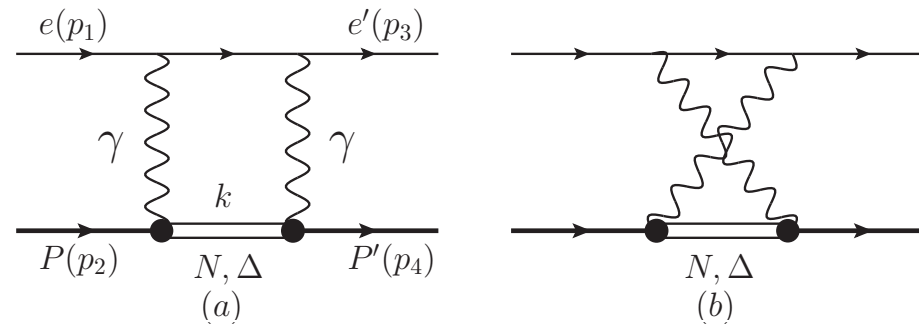


PGB, Melnitchouk, & Tjon, PRL **91**, 142304 (2003)

## Nucleon (elastic) intermediate state



# $\Delta$ and $N^*$ intermediate states



## Direct loop integration method

Kondratyuk *et al.*, PRL **95**, 172503 (2005)

Zhou & Yang, Eur. Phys. J. A. **51**, 105 (2015)

Unphysical divergence

- Include all 3  $N \rightarrow \Delta$  multipoles, with form factors fit to CLAS data
- Opposite sign to nucleon contribution
- **Qualitatively** correct, BUT diverges as  $\epsilon \rightarrow 1$ , implying a violation of unitarity (Froissart bound)

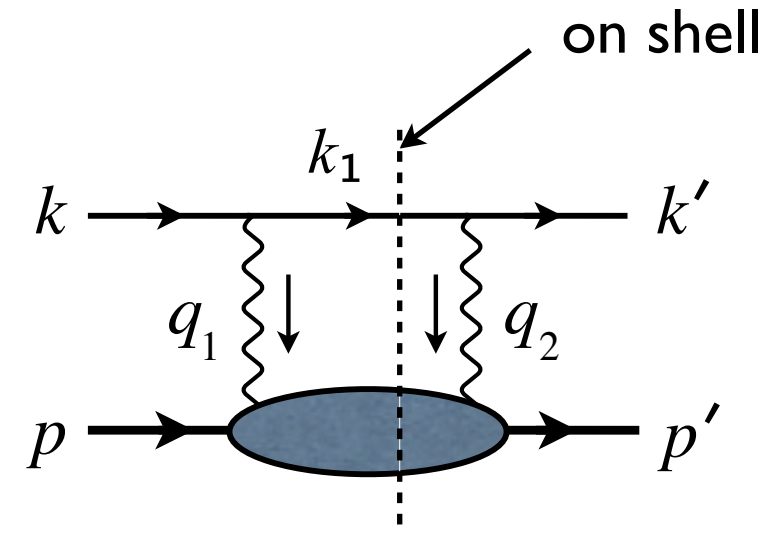


# Dispersive method

$$S = 1 + i\mathcal{M}$$

$$S^\dagger = 1 - i\mathcal{M}^\dagger$$

$$SS^\dagger = 1$$



Unitarity  $\rightarrow -i (\mathcal{M} - \mathcal{M}^\dagger) = 2\Im \mathcal{M} = \mathcal{M}^\dagger \mathcal{M}$

$$\Im \langle f | \mathcal{M} | i \rangle = \frac{1}{2} \int d\rho \sum_n \langle f | \mathcal{M}^* | n \rangle \langle n | \mathcal{M} | i \rangle$$

$$d\rho = \frac{d^3 k_1}{(2\pi)^3 2E_{k_1}} \sim dW_n dQ_1^2 dQ_2^2$$

- Imaginary part determined by unitarity
- Uses only on-shell form factors
  - Use form factors directly fit to data, not reparametrized by sum of monopoles
- Real part determined from dispersion relations

# TPE using dispersion relations

## Generalized form factors

$$\mathcal{M}_{\gamma\gamma} \rightarrow (\gamma_\mu)^{(e)} \otimes \left( F'_1(Q^2, \nu) \gamma^\mu + F'_2(Q^2, \nu) \frac{i\sigma^{\mu\nu} q_\nu}{2M} \right)^{(p)} \\ + (\gamma_\mu \gamma_5)^{(e)} \otimes (G'_a(Q^2, \nu) \gamma^\mu \gamma_5)^{(p)}$$

$$\delta_{\gamma\gamma} = 2\text{Re} \frac{\varepsilon G_E(F'_1 - \tau F'_2) + \tau G_M(F'_1 + F'_2) + \nu(1 - \varepsilon)G_M G'_a}{\varepsilon G_E^2 + \tau G_M^2}$$

## Dispersion relations

$$\text{Re } F'_1(Q^2, \nu) = \frac{2}{\pi} \mathcal{P} \int_{-\tau}^{\infty} d\nu' \frac{\nu}{\nu'^2 - \nu^2} \text{Im } F'_1(Q^2, \nu'),$$

$$\text{Re } F'_2(Q^2, \nu) = \frac{2}{\pi} \mathcal{P} \int_{-\tau}^{\infty} d\nu' \frac{\nu}{\nu'^2 - \nu^2} \text{Im } F'_2(Q^2, \nu'),$$

$$\text{Re } G'_a(Q^2, \nu) = \frac{2}{\pi} \mathcal{P} \int_{-\tau}^{\infty} d\nu' \frac{\nu'}{\nu'^2 - \nu^2} \text{Im } G'_a(Q^2, \nu').$$

Integral extends into “unphysical region” down to zero energy ( $\cos \theta < -1$ )

# A few technical details

$$\frac{\alpha}{4\pi} Q^2 \frac{1}{i\pi^2} \int d^4 q_1 \frac{\text{Im} \{ L_{\alpha\mu\nu} H^{\alpha\mu\nu} \}}{(q_1^2 - \lambda^2)(q_2^2 - \lambda^2)}$$

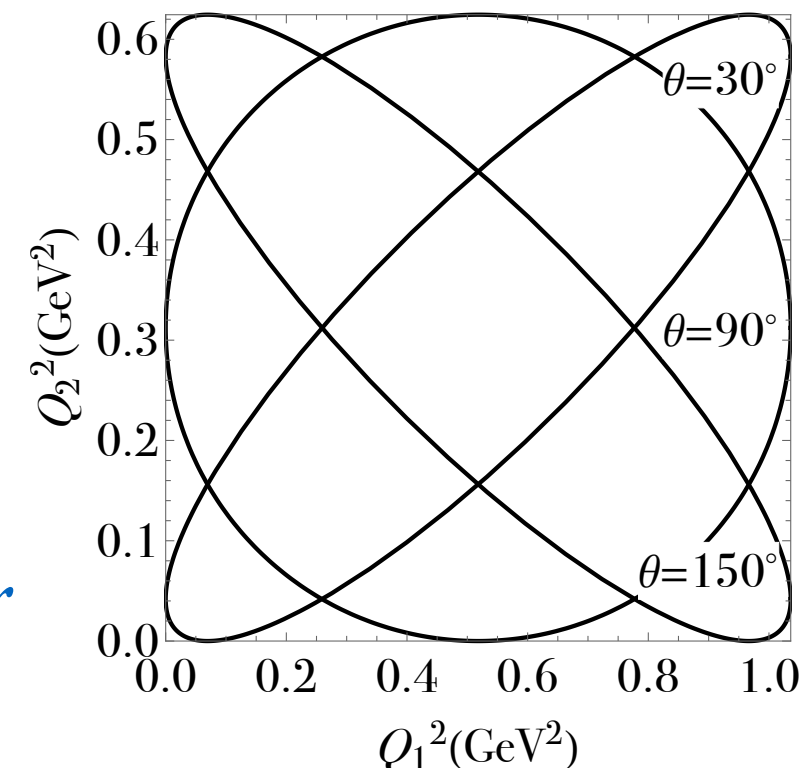
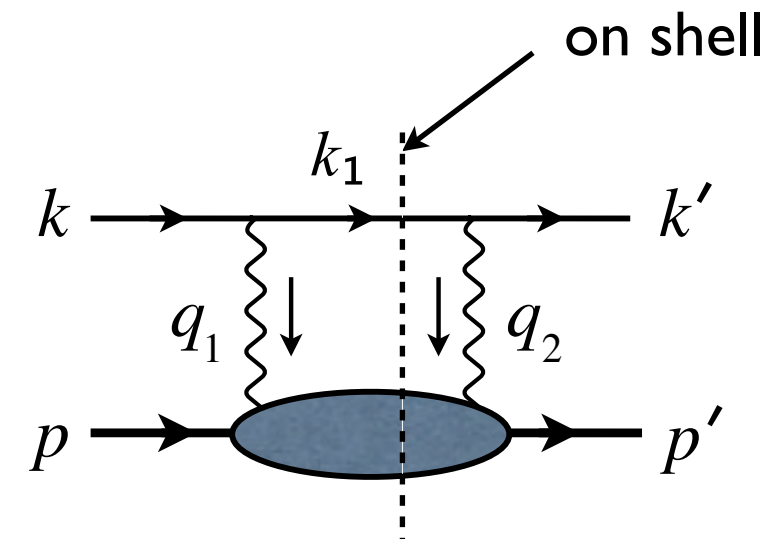
$$\rightarrow \frac{s - W^2}{4s} \int d\Omega_{k_1} \frac{f(Q_1^2, Q_2^2) G_1(Q_1^2) G_2(Q_2^2)}{(Q_1^2 + \lambda^2)(Q_2^2 + \lambda^2)}$$

- $L$  and  $H$  are leptonic and hadronic tensors
- $f$  is a polynomial in photon virtualities  $Q_1^2$  and  $Q_2^2$
- $G_i(Q_i^2)$  is a transition form factor with poles in the complex  $Q_i^2$  plane

Use numerical contour integration

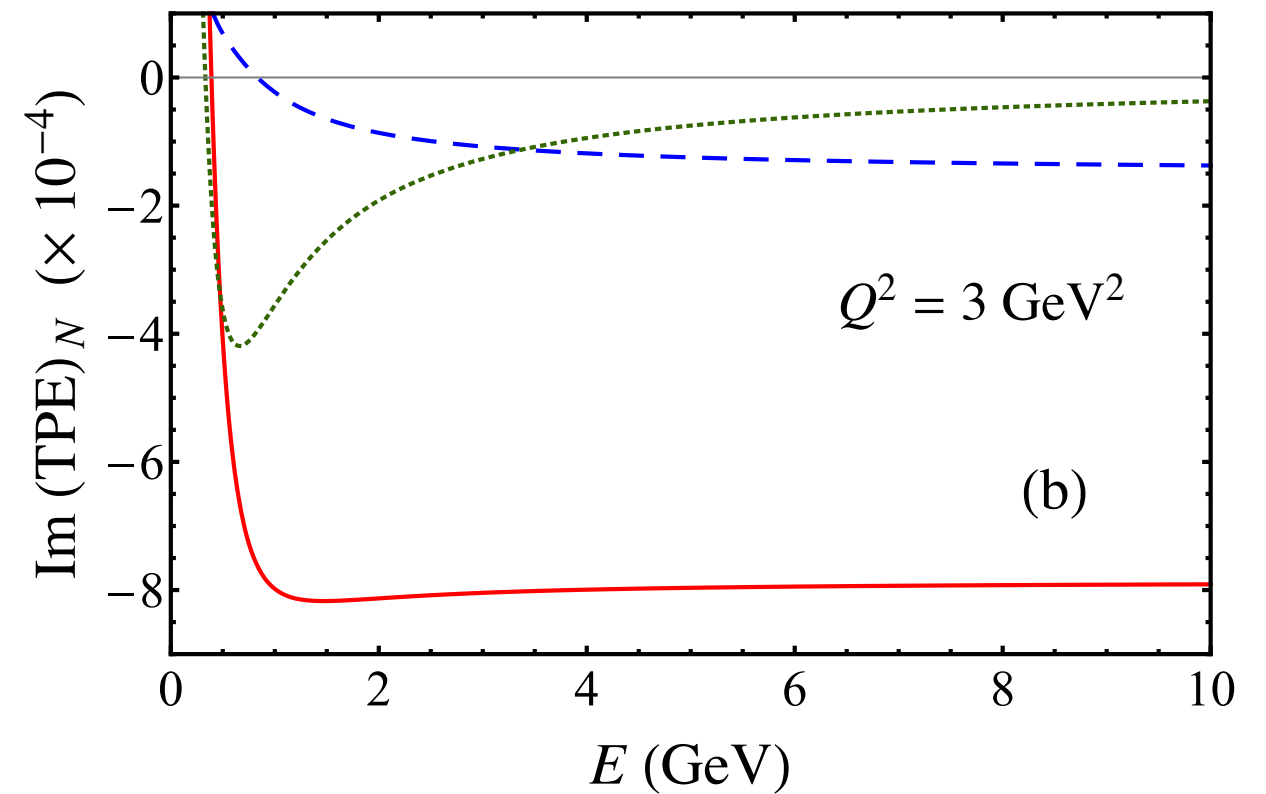
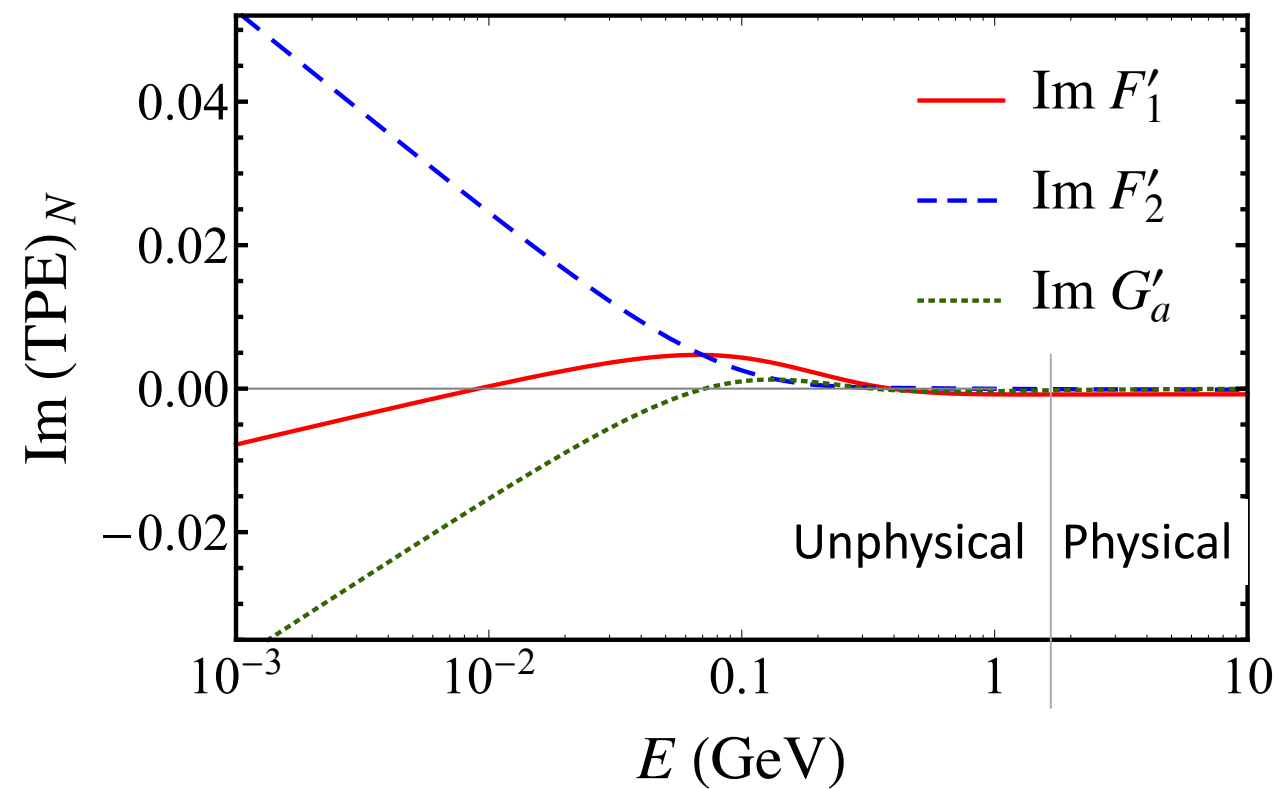
→ Allows for use of arbitrary functional forms for transition form factors  $G_i(Q_i^2)$

Contours are concentric ellipses of radial parameter  $r$



# Nucleon (elastic) intermediate state

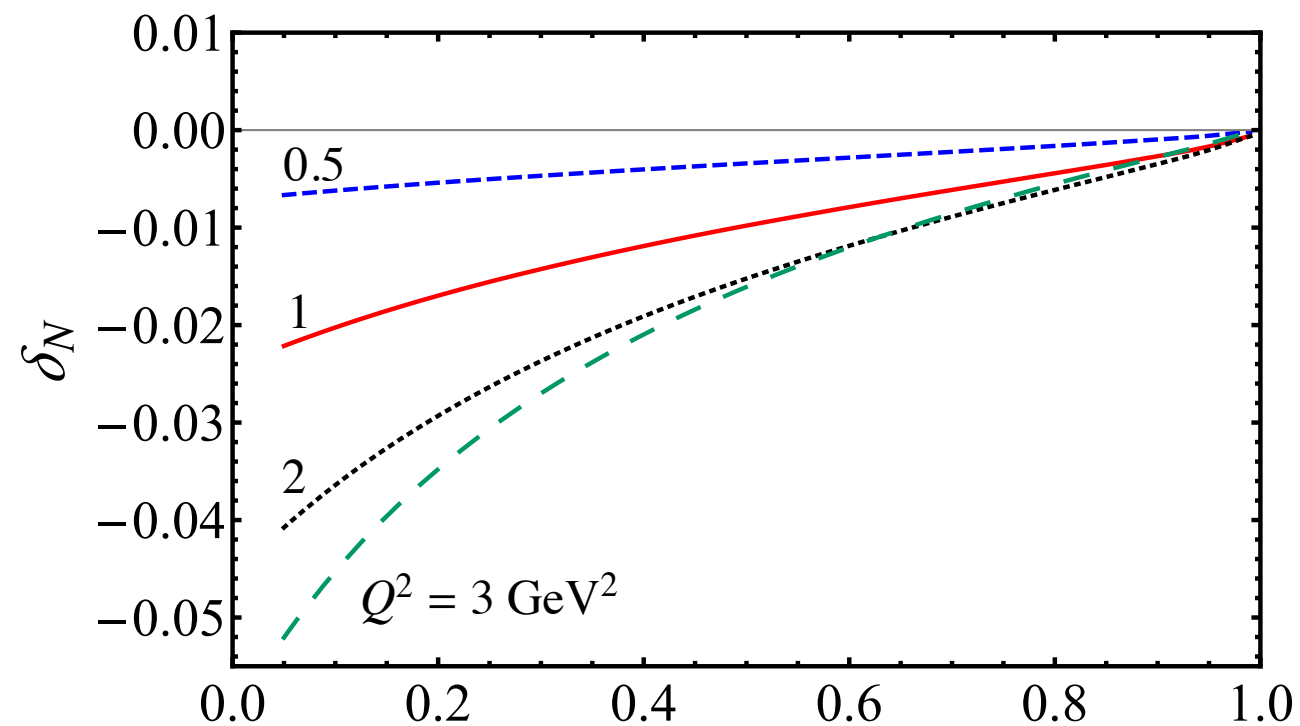
$$Q^2 = 3 \text{ GeV}^2$$



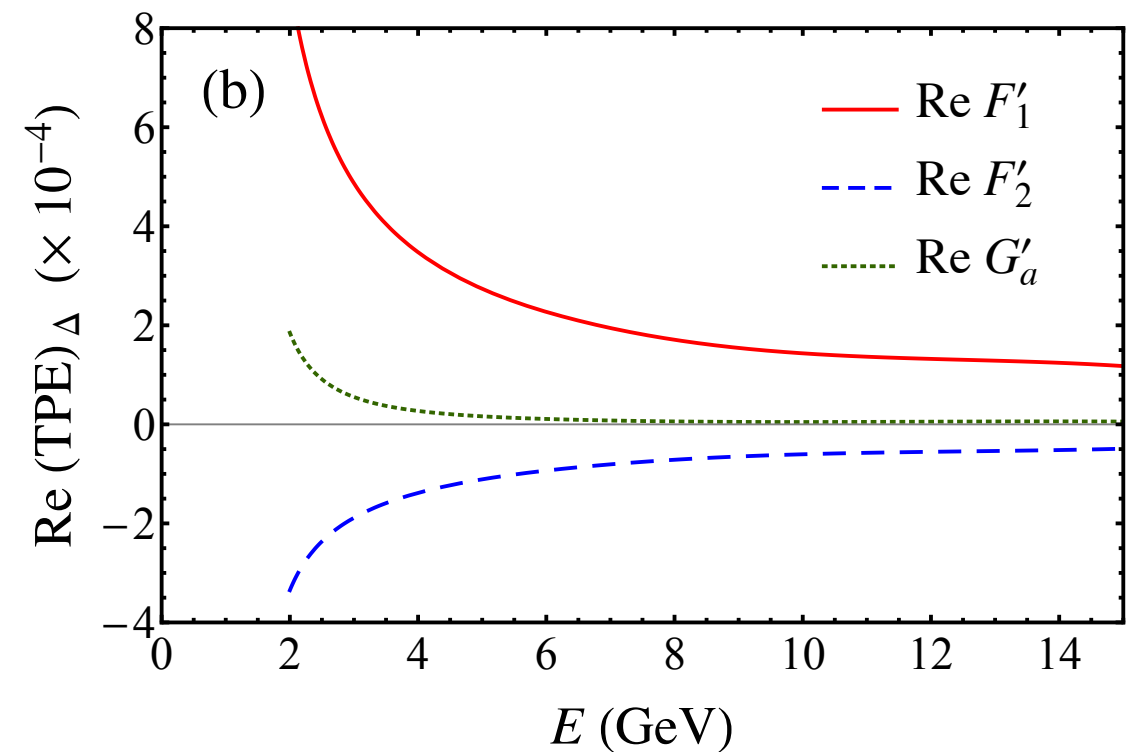
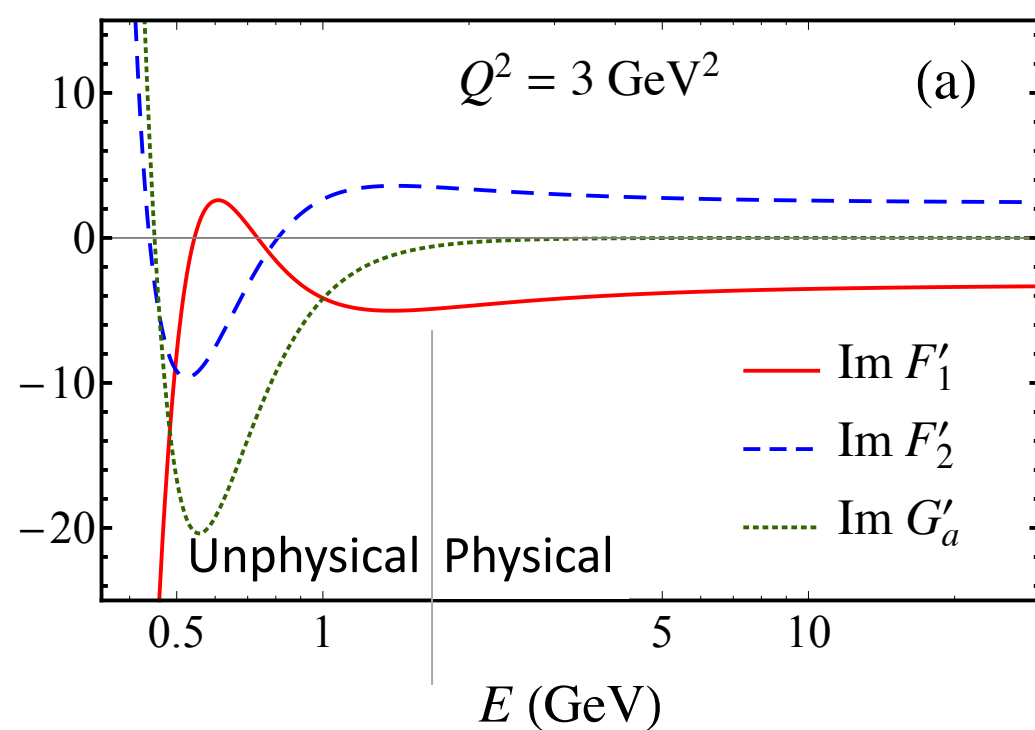
Logarithmic divergence  
at low energies

No subtractions needed

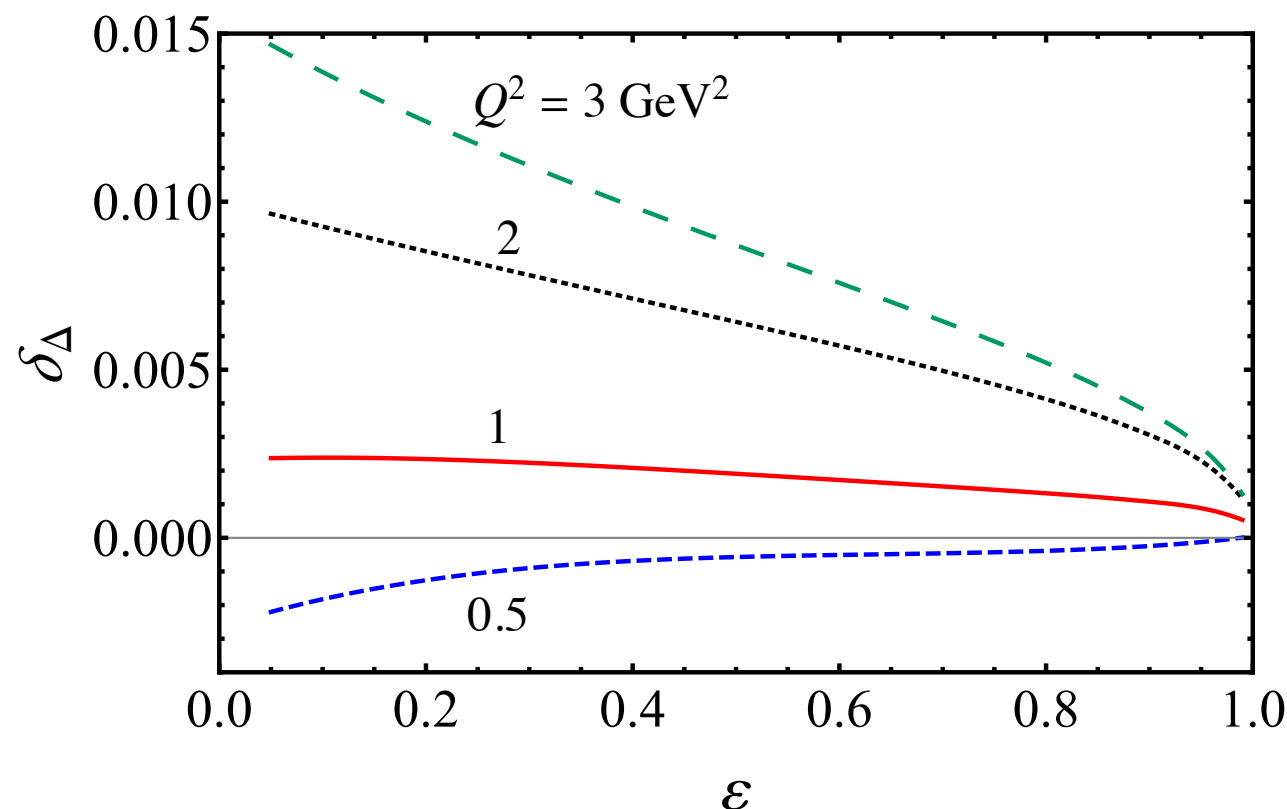
Agrees with old loop  
integration method



# $\Delta$ intermediate state (zero width approximation)



- Include all 3 multipoles, with form factors fit to recent CLAS data
- $G_M^* \times G_M^*$  dominates, but  $G_M^* \times G_E^*$  interference is significant



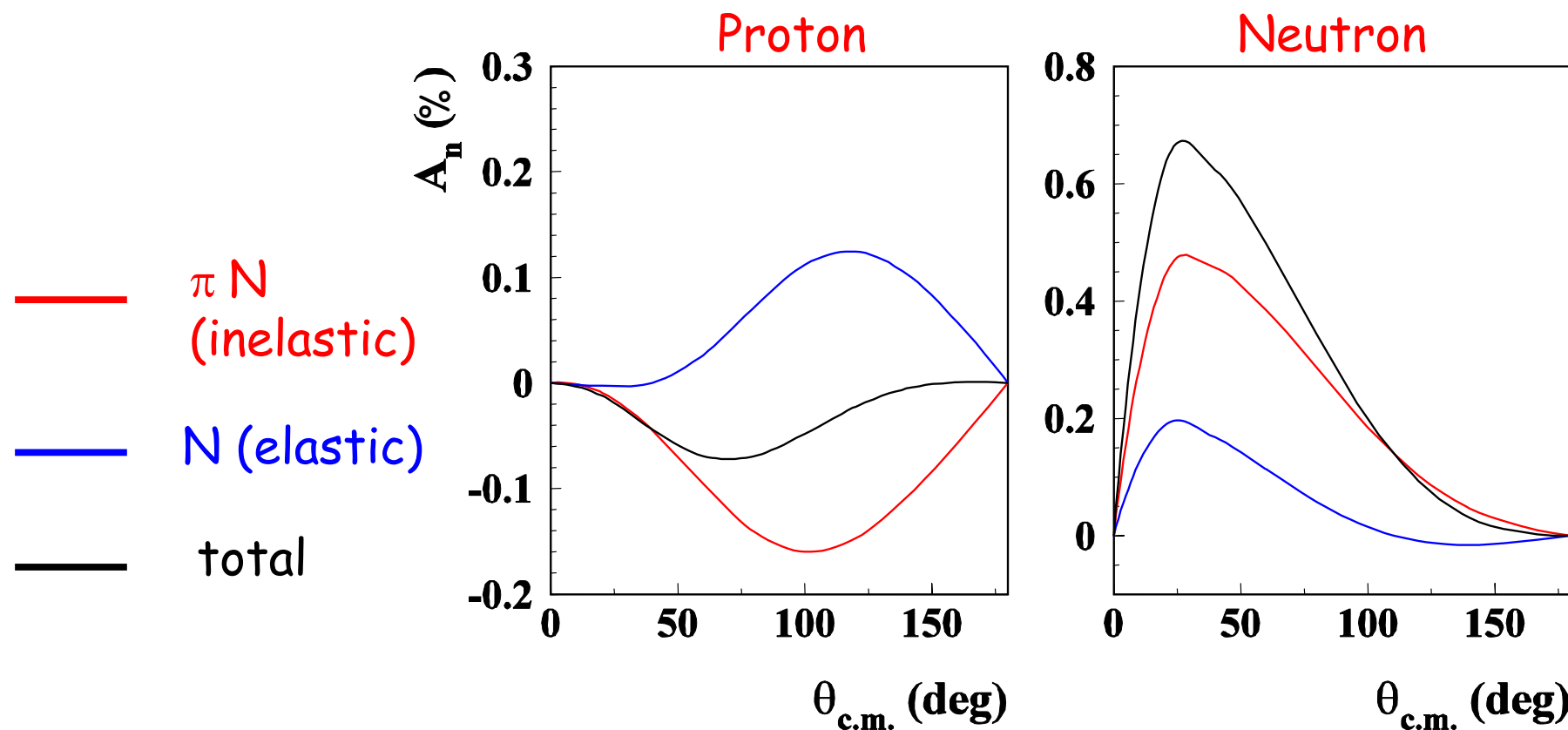
No unphysical  
divergence at  $\epsilon \rightarrow 1$

changes sign at  $Q^2 \approx 0.6 \text{ GeV}^2$

# Direct measurements of Im part

Target normal spin asymmetry

$E_e = 0.570 \text{ GeV}$



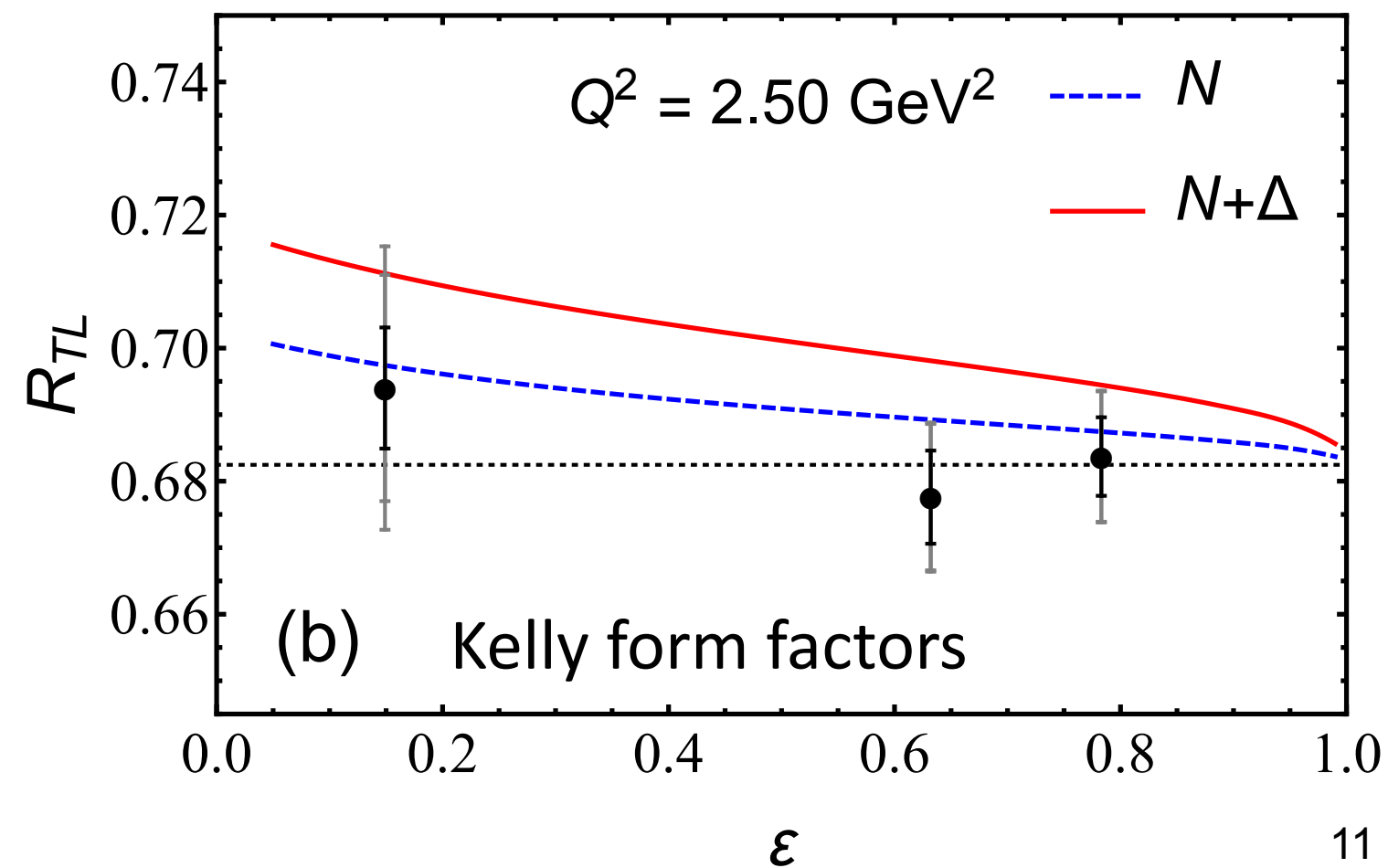
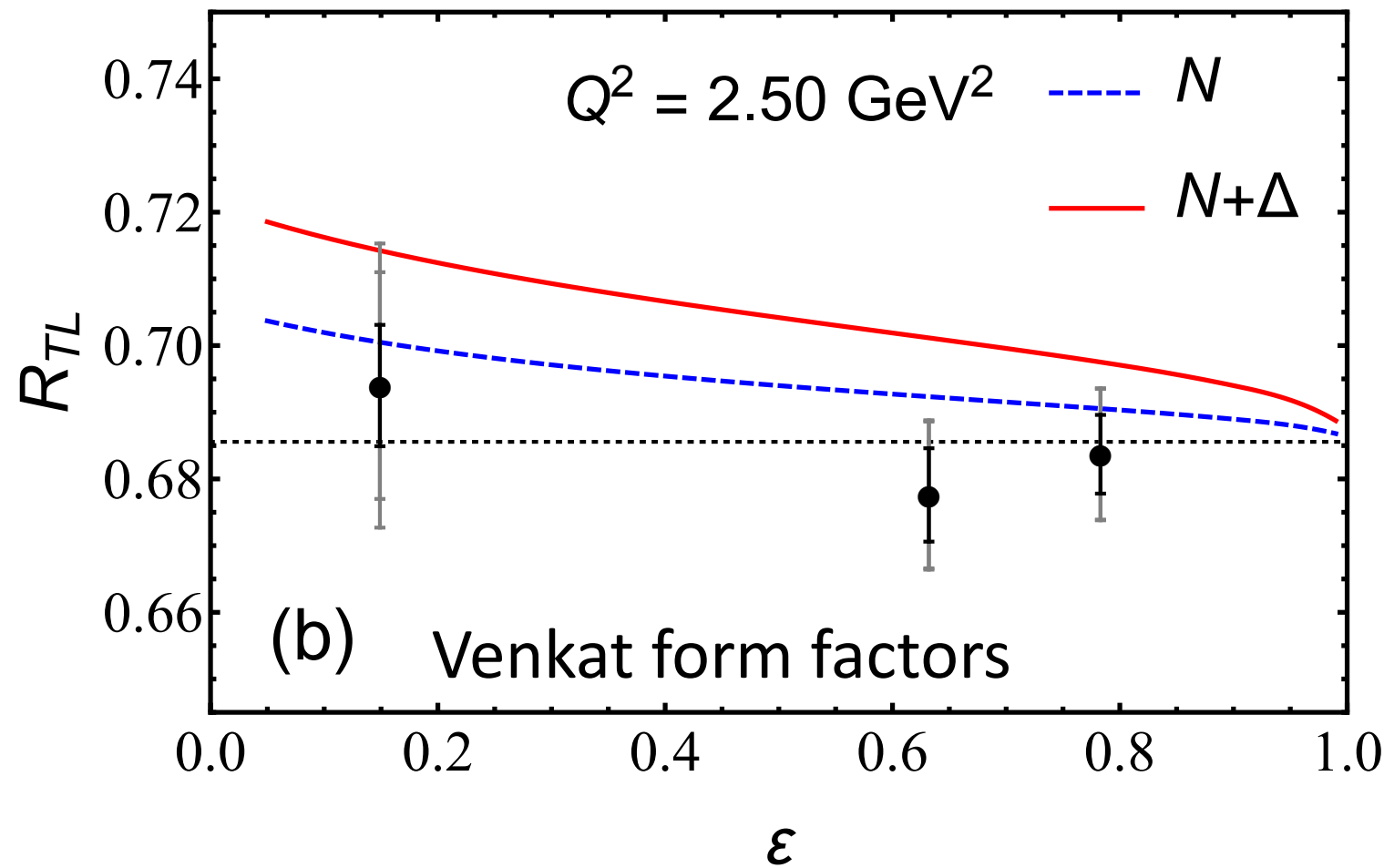
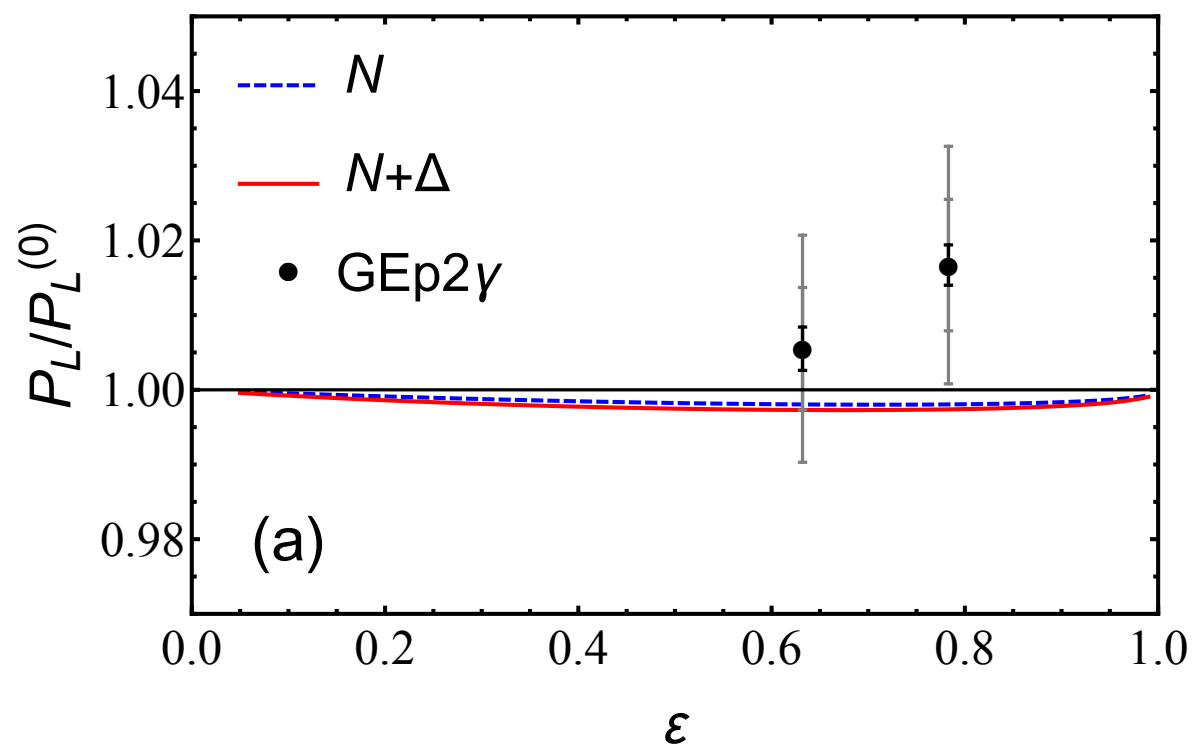
(taken from Pasquini & Vanderhaeghen)

$$A_n = \sqrt{\frac{2\varepsilon(1+\varepsilon)}{\tau}} \left( G_M^2 + \frac{\varepsilon}{\tau} G_E^2 \right)^{-1} \times \left\{ -G_M \text{Im} \left( \delta \tilde{G}_E + \frac{\nu}{M^2} \tilde{F}_3 \right) + G_E \text{Im} \left( \delta \tilde{G}_M + \left( \frac{2\varepsilon}{1+\varepsilon} \right) \frac{\nu}{M^2} \tilde{F}_3 \right) \right\}$$

This is all in the physical region.

# Polarization data

$R_{TL}$  indicates mild sensitivity to  $G_E$  form factor at low  $\varepsilon$

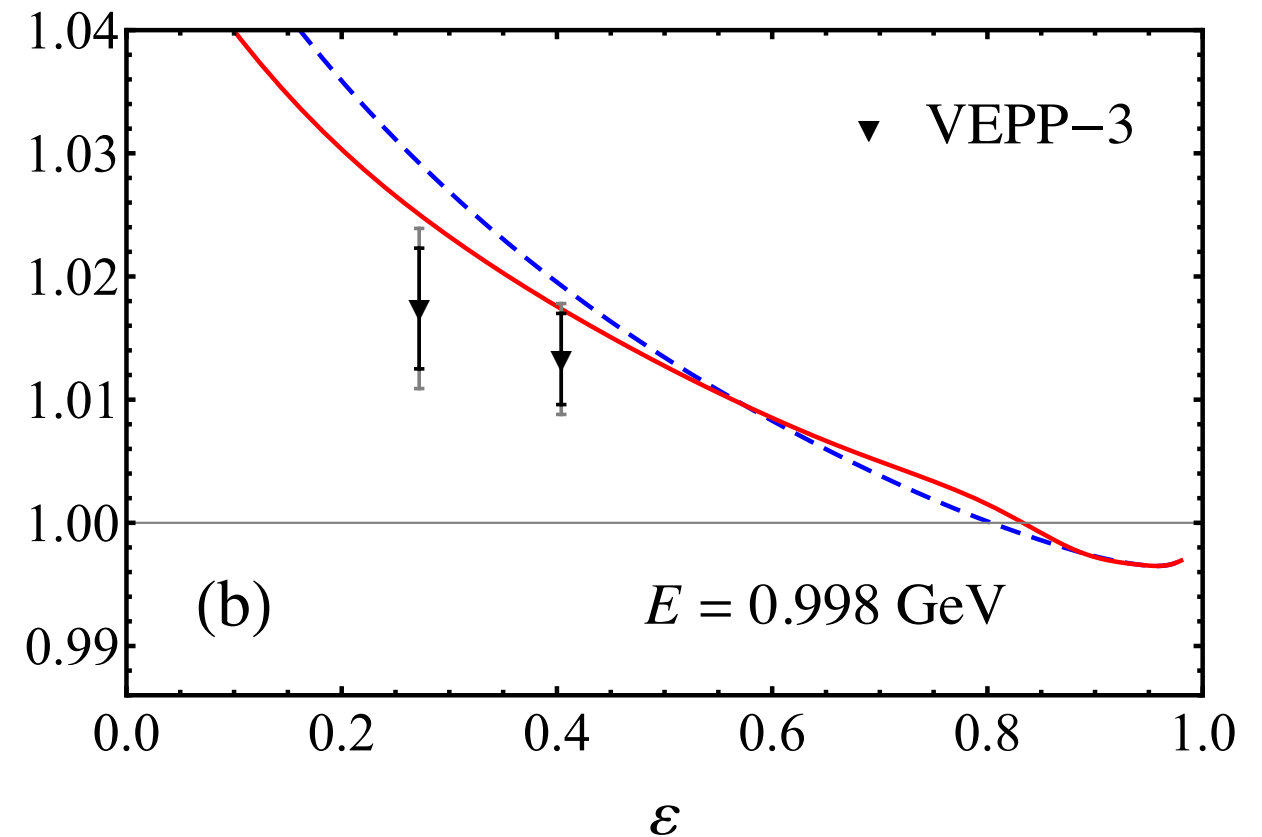
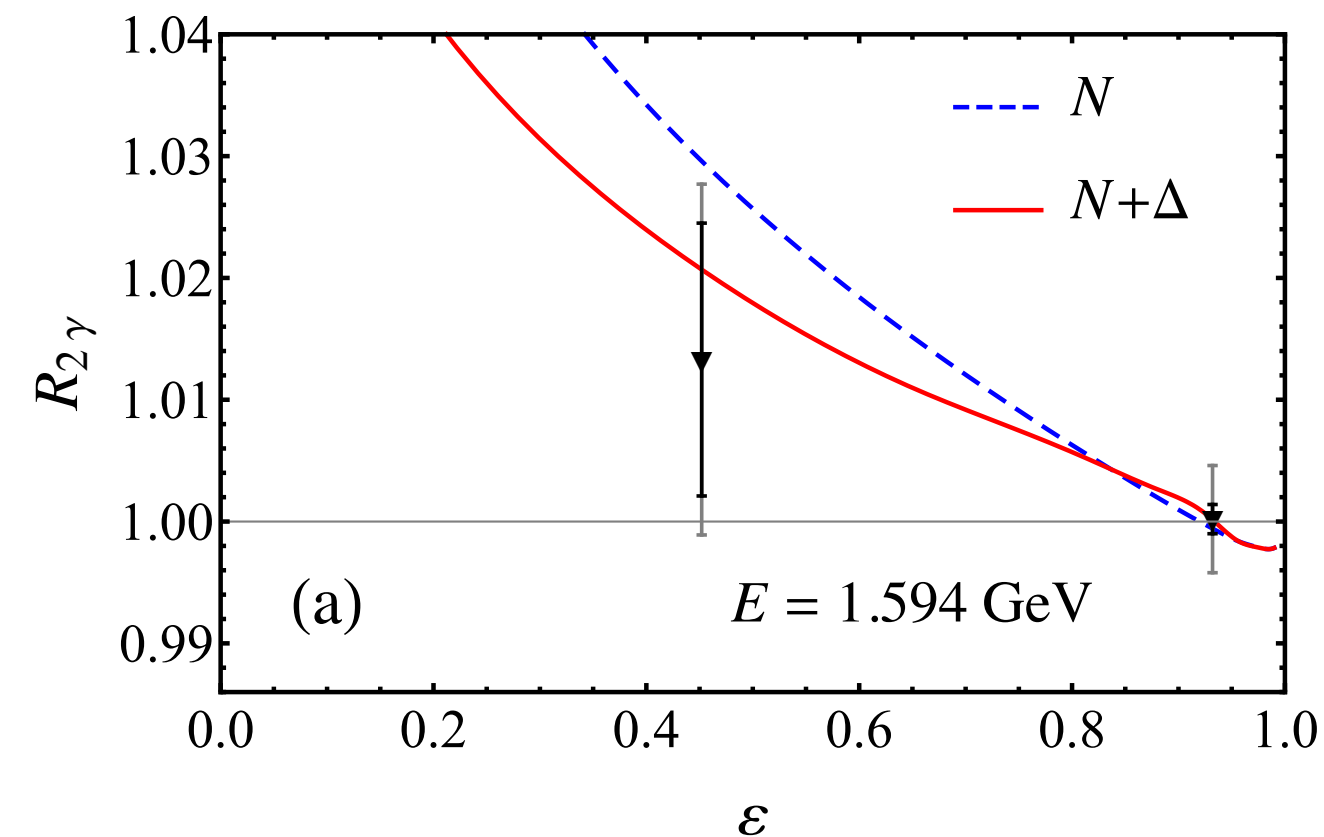


# TPE effect on ratio of $e^+p$ to $e^-p$ cross sections

TPE interference changes sign for positrons vs electrons

$$R_{2\gamma} = \frac{\sigma^{e^+}}{\sigma^{e^-}} \approx 1 - 2\delta_{\gamma\gamma}$$

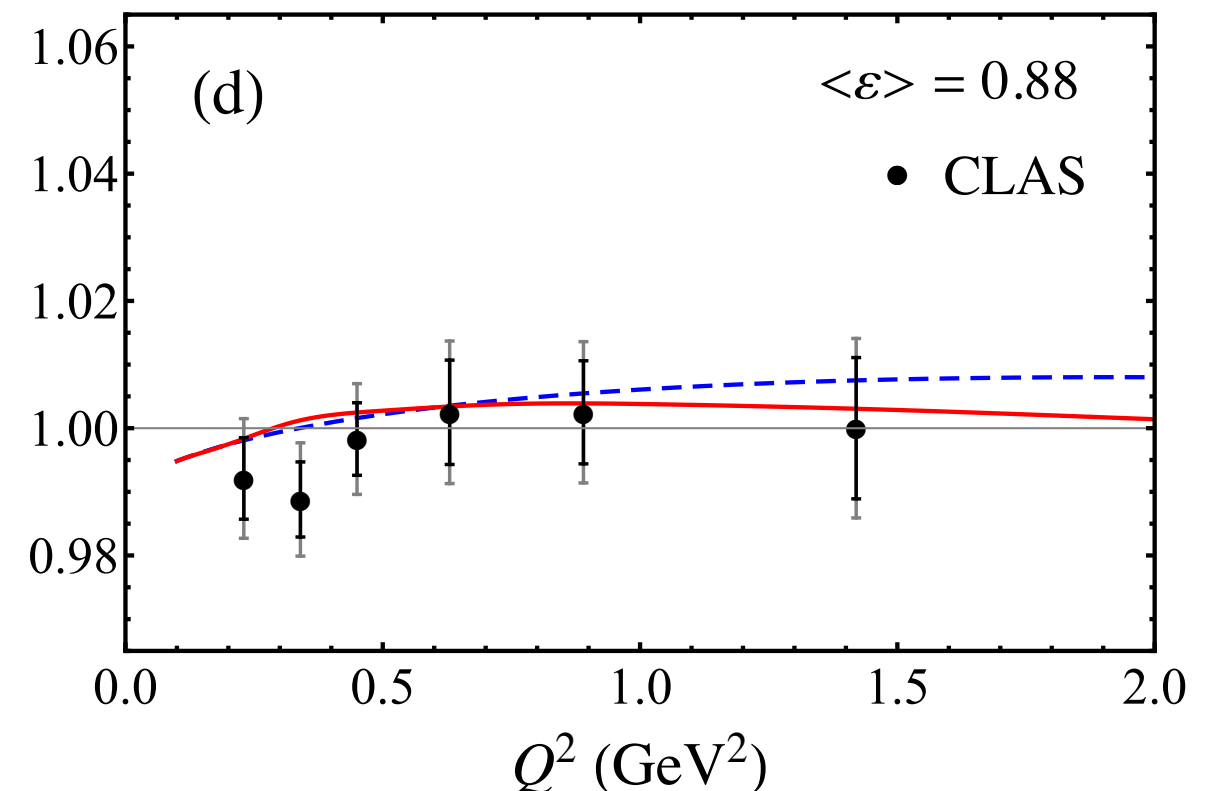
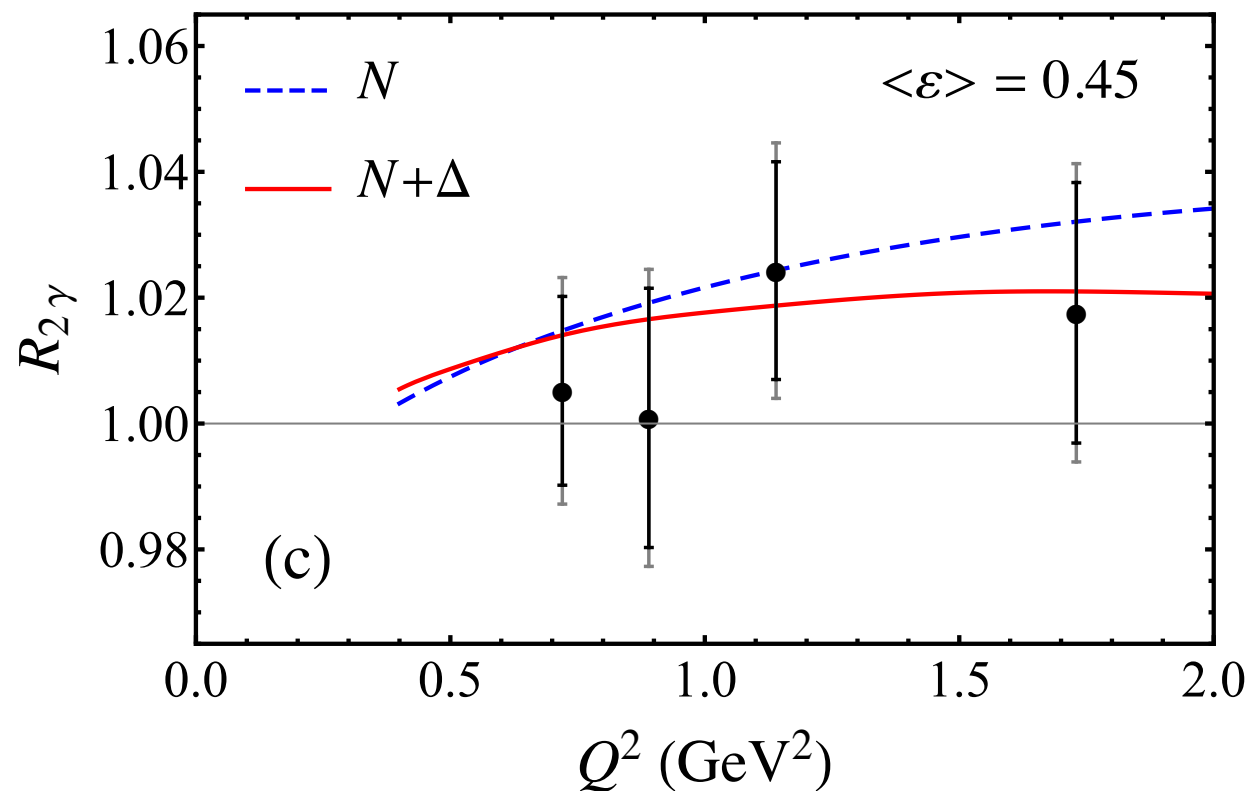
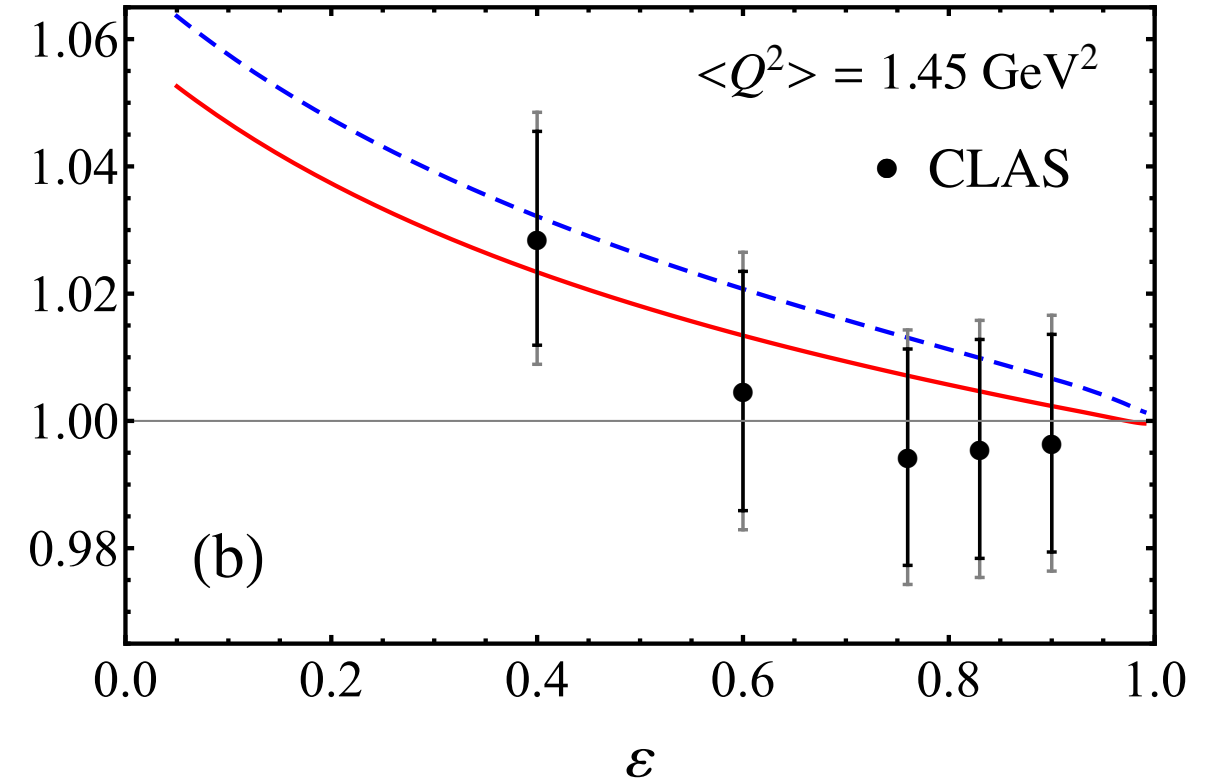
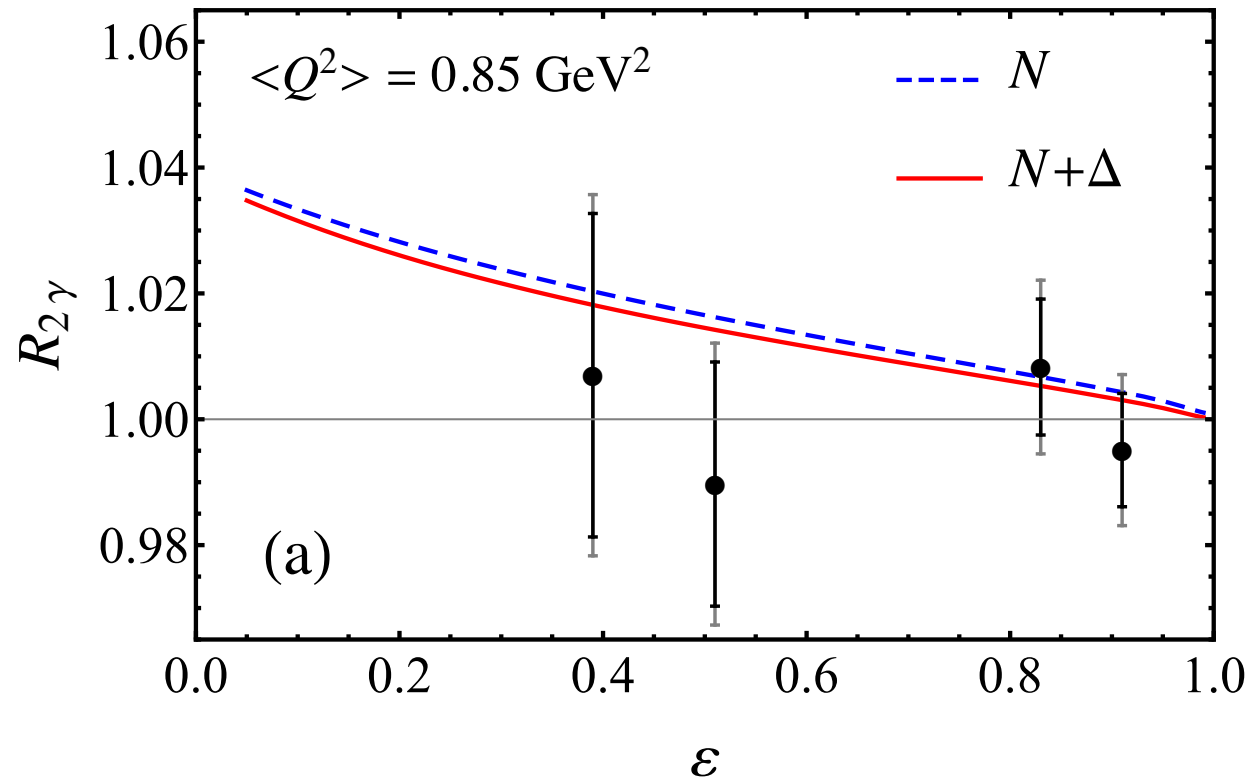
VEPP-3 (Novosibirsk)





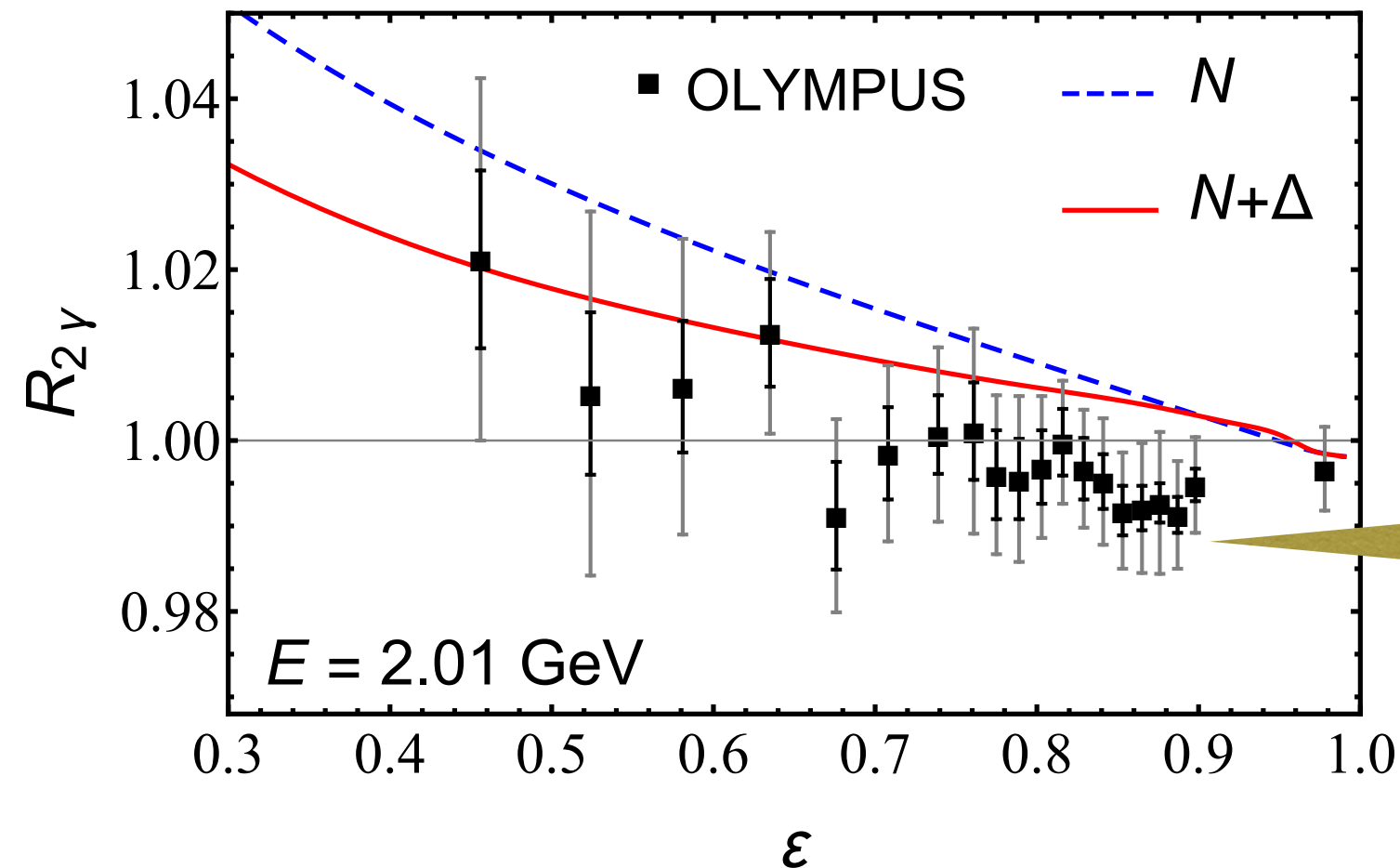
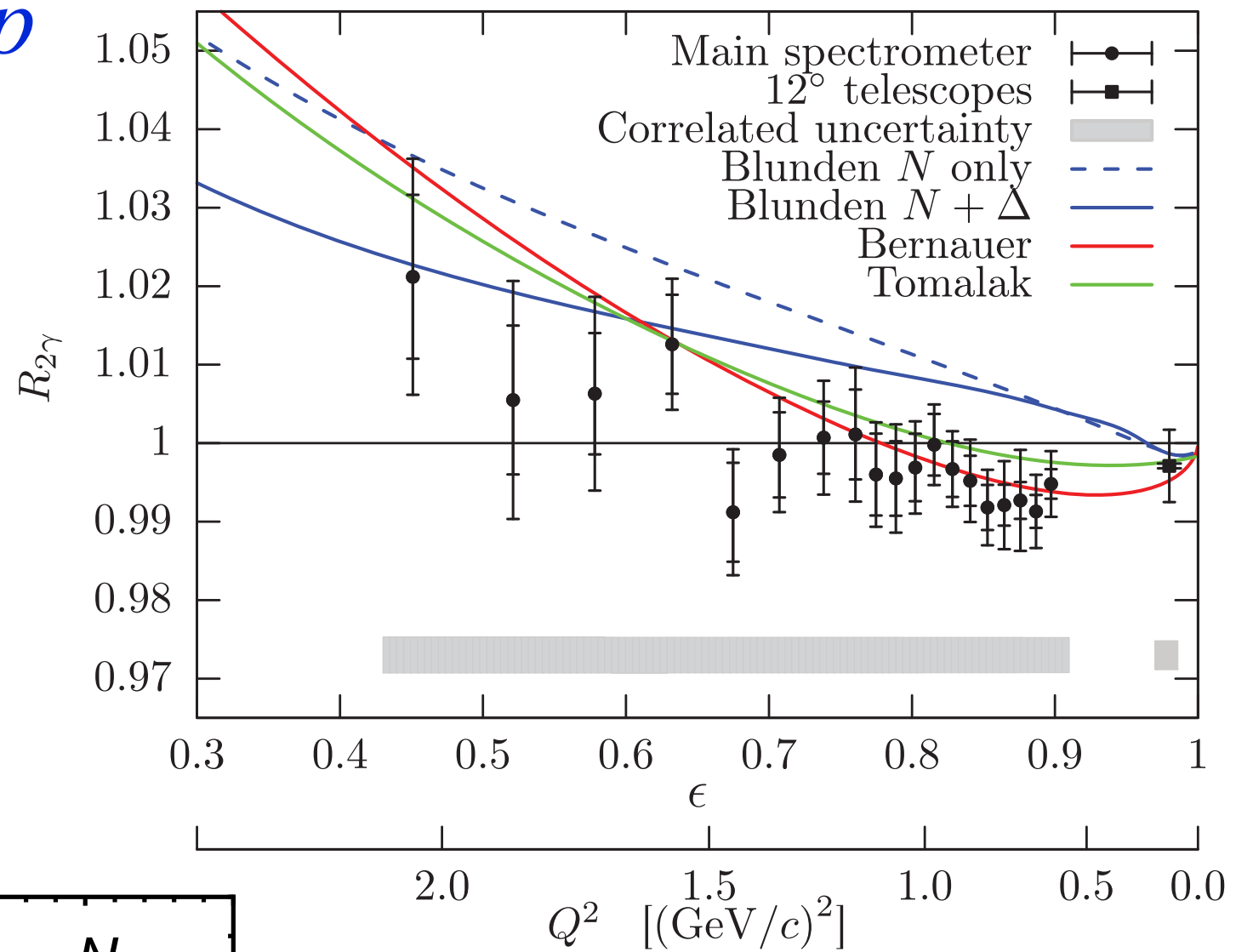
# TPE effect on ratio of $e^+p$ to $e^-p$ cross sections

## CLAS (Jefferson Lab)



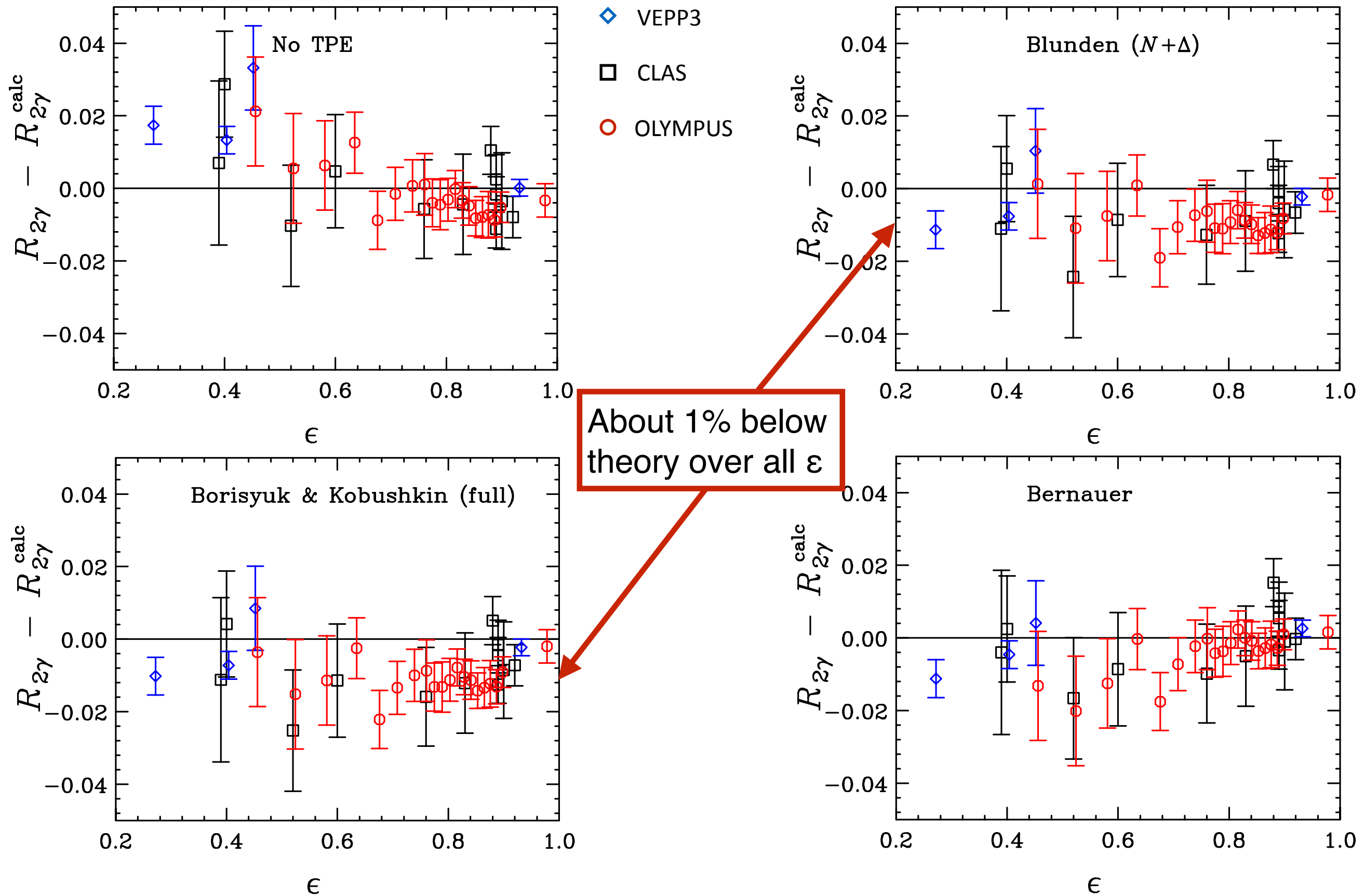
# TPE effect on ratio of $e^+p$ to $e-p$ cross sections

OLYMPUS  
(Doris ring @ DESY)

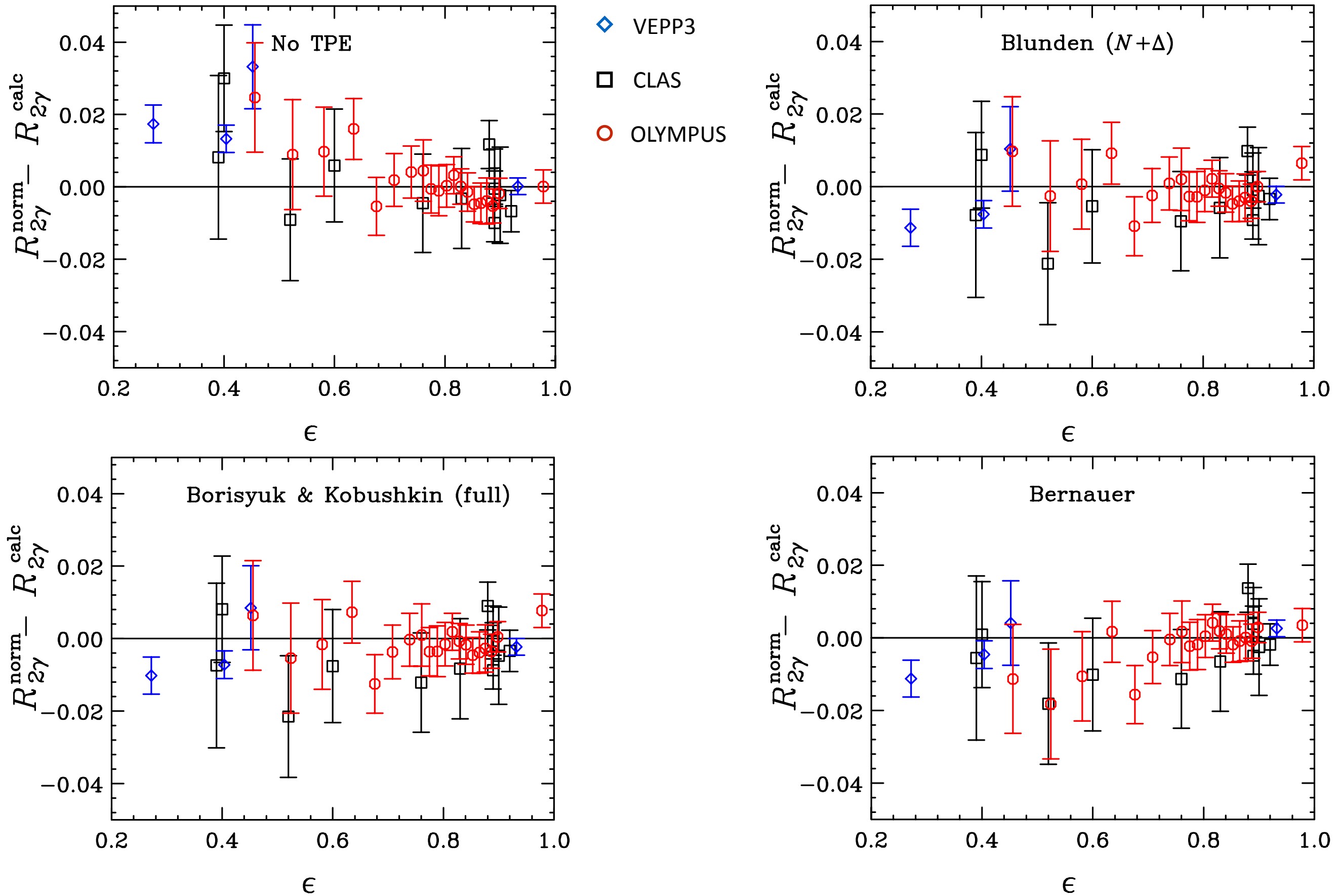


What is going on  
at low  $Q^2$ ?

# Comparing theory and experiment



# Allowing normalization to float



# Correction to proton weak charge

- including one-loop radiative corrections

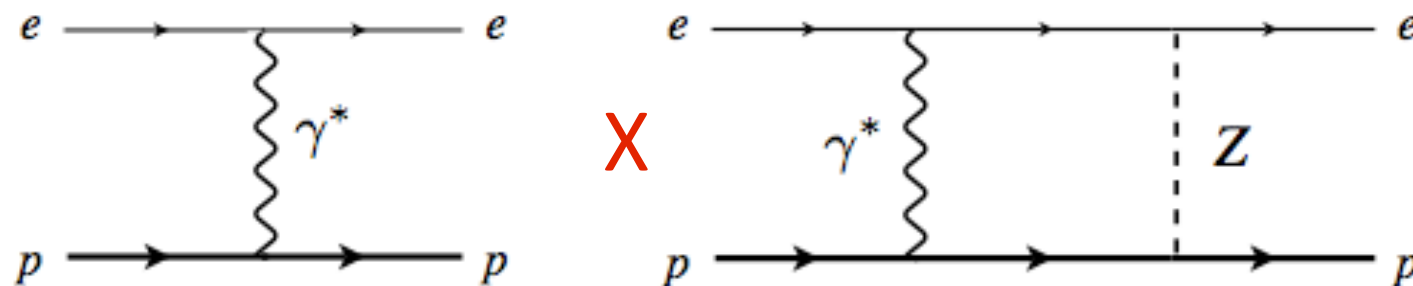
$$Q_W^p = \rho \left( 1 - 4\kappa_{\text{PT}}(0)\hat{s}^2 + \Delta'_e + \Delta_W \right)$$

$$+ \square_{WW} + \square_{ZZ} + \square_{\gamma Z}$$

e.w. vertex  
corrections

box diagrams

Box corrections



→  $WW$  and  $ZZ$  box diagrams large but dominated by short distances; can be evaluated perturbatively

→  $\gamma Z$  box diagram sensitive to long distance physics, has two contributions:

$$\square_{\gamma Z} = \square_{\gamma Z}^A + \square_{\gamma Z}^V$$

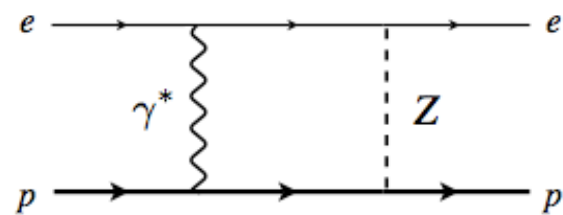
$V(e) \times A(h)$   
(finite at  $E=0$ )

$A(e) \times V(h)$   
(inelastic vanishes at  $E=0$ )

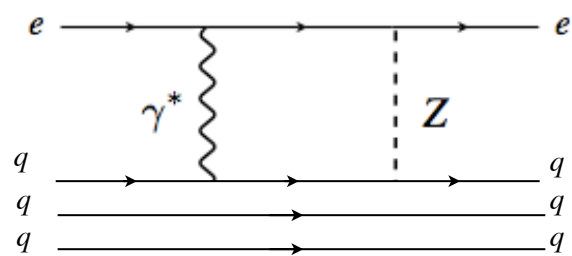
# Axial $h$ correction

- axial  $h$  correction  $\square_{\gamma Z}^A$  dominant  $\gamma Z$  correction in atomic parity violation at very low (zero) energy

→ computed by Marciano & Sirlin in 1983 as sum of two parts:



- ★ low-energy part approximated by *Born* contribution (elastic intermediate state)



- ★ high-energy part (above scale  $\Lambda \sim 1$  GeV) computed perturbatively in terms of scattering from *free quarks*

$$\square_{\gamma Z}^A = (1 - 4\hat{s}^2) \underbrace{\frac{5\alpha}{2\pi} \int_{\Lambda^2}^{\infty} \frac{dQ^2}{Q^2(1 + Q^2/M_Z^2)} \left(1 - \frac{\alpha_s(Q^2)}{\pi}\right)}_{\sim \log \frac{M_Z^2}{\Lambda^2} + c}$$

# Forward angle dispersion method

Gorchtein, Horowitz, PRL 102 (2009) 091806

$$S = 1 + i\mathcal{M}$$

$$S^\dagger = 1 - i\mathcal{M}^\dagger$$

$$SS^\dagger = 1$$

$$\text{Unitarity} \rightarrow -i(\mathcal{M} - \mathcal{M}^\dagger) = 2\Im m \mathcal{M} = \mathcal{M}^\dagger \mathcal{M}$$

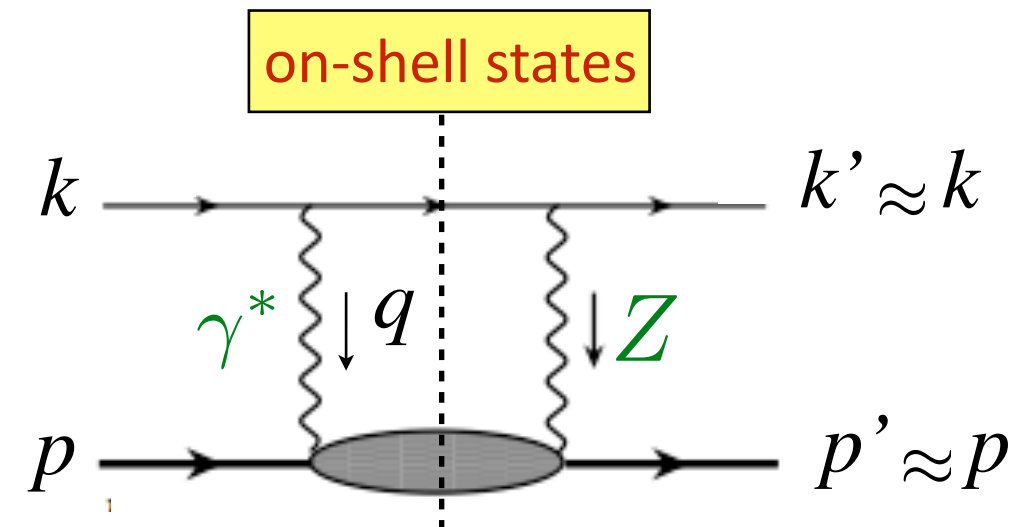
$$\Im m \langle f | \mathcal{M} | i \rangle = \frac{1}{2} \int d\rho \sum_n \langle f | \mathcal{M}^* | n \rangle \langle n | \mathcal{M} | i \rangle$$

Forward scattering amplitude:  $|f\rangle \approx |i\rangle$

$$\Im m \langle i | \mathcal{M} | i \rangle = \frac{1}{2} \int d\rho \sum_n |\langle n | \mathcal{M} | i \rangle|^2 \sim \int d^3 k_1 \frac{L_{\mu\nu} W^{\mu\nu}}{q^2 (q^2 - M_Z^2)}$$

hadronic tensor:

$$MW_{\gamma Z}^{\mu\nu} = -g^{\mu\nu} \underbrace{\text{vector } h}_{\text{vector } h} \left( F_1^{\gamma Z} \right) + \frac{p^\mu p^\nu}{p \cdot q} \underbrace{\text{vector } h}_{\text{vector } h} \left( F_2^{\gamma Z} \right) - i\epsilon^{\mu\nu\lambda\rho} \frac{p_\lambda q_\rho}{2p \cdot q} \underbrace{\text{axial } h}_{\text{axial } h} \left( F_3^{\gamma Z} \right)$$



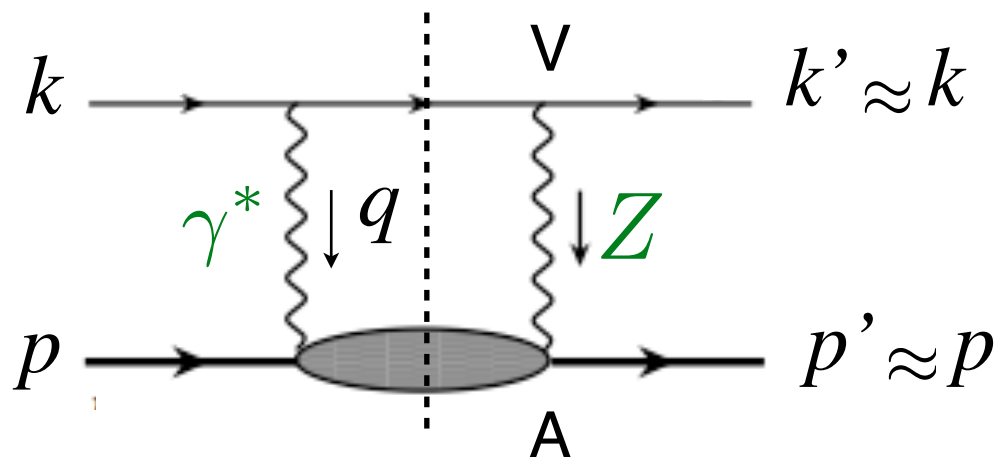
## Axial $h$ correction

- At low energy, dominant  $V_e \times A_h$  correction evaluated using forward dispersion relations

$$\Re \square_{\gamma Z}^A(E) = \frac{2}{\pi} \int_0^\infty dE' \frac{E'}{E'^2 - E^2} \Im \square_{\gamma Z}^A(E')$$

→ imaginary part given by  $F_3^{\gamma Z}$  structure function

$$\begin{aligned} \Im \square_{\gamma Z}^A(E) = & \frac{1}{(2ME)^2} \int_{M^2}^s dW^2 \int_0^{Q_{\max}^2} dQ^2 \frac{v_e(Q^2) \alpha(Q^2)}{1 + Q^2/M_Z^2} \\ & \times \left( \frac{2ME}{W^2 - M^2 + Q^2} - \frac{1}{2} \right) \left( F_3^{\gamma Z} \right) \end{aligned}$$



with  $v_e(Q^2) = 1 - 4\kappa(Q^2)\hat{s}^2$



# Axial $h$ correction DIS part (dominant contribution)

- DIS part dominated by leading twist PDFs at small  $x$   
(MSTW, CTEQ, Alekhin parametrizations)

$$F_3^{\gamma Z(\text{DIS})}(x, Q^2) = \sum_q 2 e_q g_A^q (q(x, Q^2) - \bar{q}(x, Q^2))$$

→ in DIS region ( $Q^2 \gtrsim 1 \text{ GeV}^2$ ), expand integrand in powers of  $x$

$$\Re \Pi_{\gamma Z}^{\text{A(DIS)}}(E) = \frac{3}{2\pi} \int_{Q_0^2}^{\infty} dQ^2 \frac{v_e(Q^2) \alpha(Q^2)}{Q^2 (1 + Q^2/M_Z^2)} \\ \times \left[ M_3^{(1)}(Q^2) + \frac{2M^2}{9Q^4} (5E^2 - 3Q^2) M_3^{(3)}(Q^2) + \dots \right]$$

with moments  $M_3^{\gamma Z(n)} = \int_0^1 dx x^{n-1} F_3^{\gamma Z}(x, Q^2)$

# Axial $h$ correction

## ■ structure function moments

$$\underline{n=1} \quad M_3^{\gamma Z(1)}(Q^2) = \frac{5}{3} \left( 1 - \frac{\alpha_s(Q^2)}{\pi} \right)$$

→  $\gamma Z$  analog of Gross-Llewellyn Smith sum rule

$$\mathcal{R}e \square_{\gamma Z}^{A(\text{DIS})} \approx (1 - 4\hat{s}^2) \frac{5\alpha}{2\pi} \int_{Q_0^2}^{\infty} \frac{dQ^2}{Q^2(1+Q^2/M_Z^2)} \left( 1 - \frac{\alpha_s(Q^2)}{\pi} \right)$$

→ precisely result from Marciano & Sirlin!  $\sim \log \frac{M_Z^2}{Q_0^2}$   
(works because result depends on lowest moment of  
*valence* PDF, with model-independent normalization!)

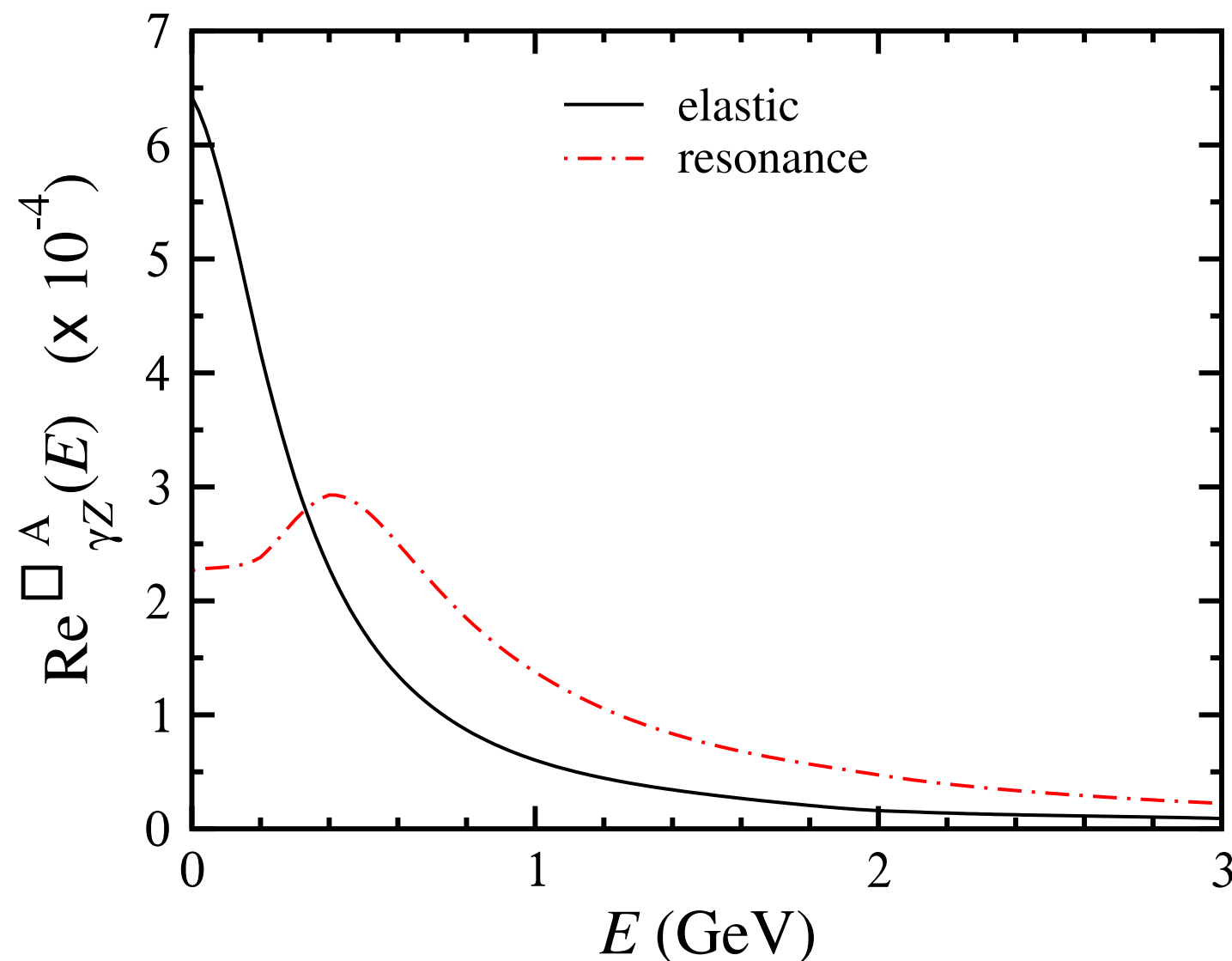
$$\underline{n=3} \quad M_3^{\gamma Z(3)}(Q^2) = \frac{1}{3} (2\langle x^2 \rangle_u + \langle x^2 \rangle_d) \left( 1 + \frac{5\alpha_s(Q^2)}{12\pi} \right)$$

→ related to  $x^2$ -weighted moment of valence quarks

# Axial $h$ elastic + resonance correction

- ★ elastic part:  $F_3^{\gamma Z(\text{el})}(Q^2) = -Q^2 G_M^p(Q^2) G_A^Z(Q^2) \delta(W^2 - M^2)$
- ★ resonance part from parametrization of  $\nu$  scattering data; includes lowest four spin 1/2 and 3/2 states (Lalakulich-Paschos)

→ Least well-constrained part of the calculation



## Vector $h$ correction

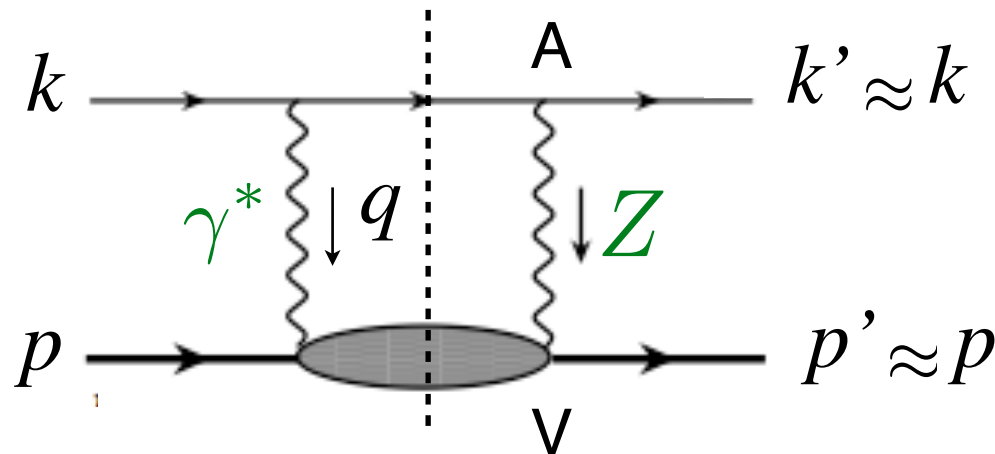
- vector  $h$  correction  $\square_{\gamma Z}^V$  vanishes at  $E = 0$ , but experiment has  $E \sim 1$  GeV - what is energy dependence?

→ forward dispersion relation

$$\Re \square_{\gamma Z}^V(E) = \frac{2E}{\pi} \int_0^\infty dE' \frac{1}{E'^2 - E^2} \Im \square_{\gamma Z}^V(E')$$

→ imaginary part given by

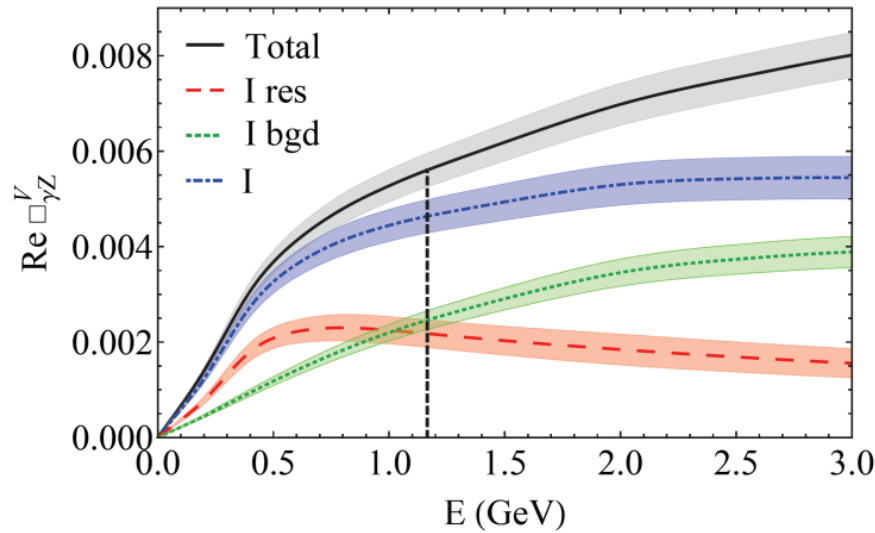
$$\Im \square_{\gamma Z}^V(E) = \frac{\alpha}{(s - M^2)^2} \int_{W_\pi^2}^s dW^2 \int_0^{Q_{\max}^2} \frac{dQ^2}{1 + Q^2/M_Z^2} \times \left( F_1^{\gamma Z} + F_2^{\gamma Z} \frac{s(Q_{\max}^2 - Q^2)}{Q^2(W^2 - M^2 + Q^2)} \right)$$



# 3 groups doing independent analyses

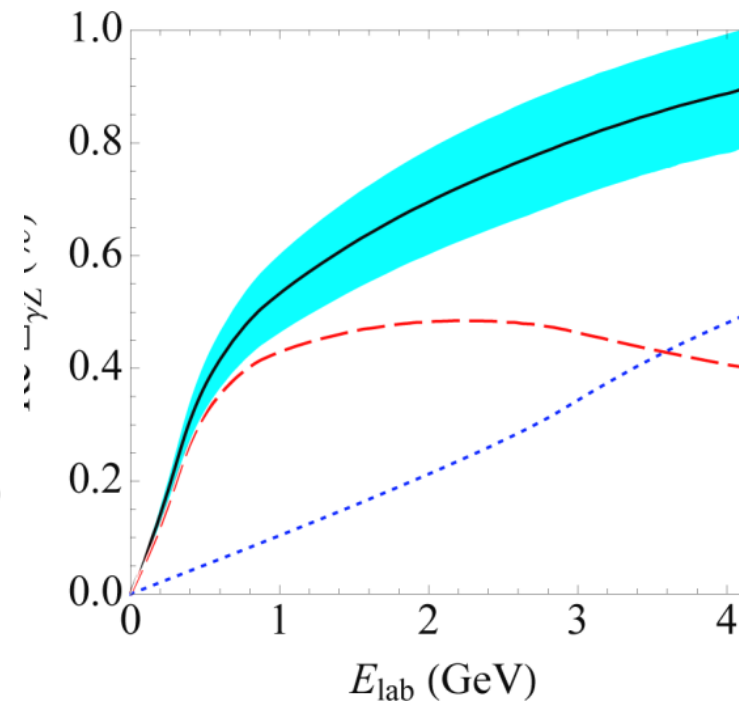
Hall *et al.*

PRD 88, 013011 (2013)



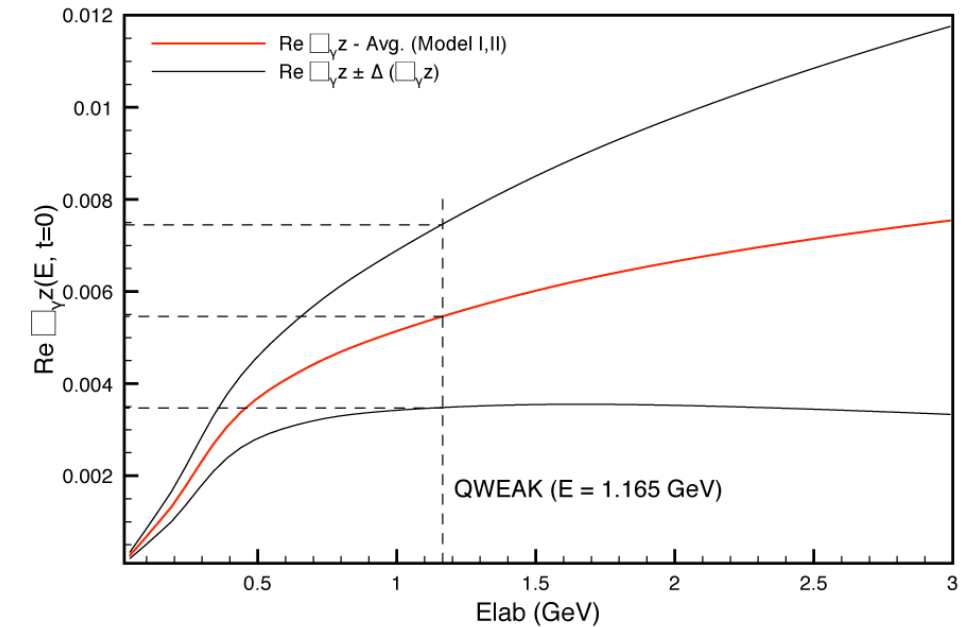
Carlson and Rislow

PRD 83, 113007 (2011)



Gorchtein *et al.*

PRC 84, 015502 (2011)



**Qweak energy:**  $\text{Re } \Pi_{\gamma Z}^V(E = 1.165 \text{ GeV})$  **8% correction!**

$(5.6 \pm 0.36) \times 10^{-3}$	$(5.7 \pm 0.9) \times 10^{-3}$	$(5.4 \pm 2.0) \times 10^{-3}$
---------------------------------	--------------------------------	--------------------------------

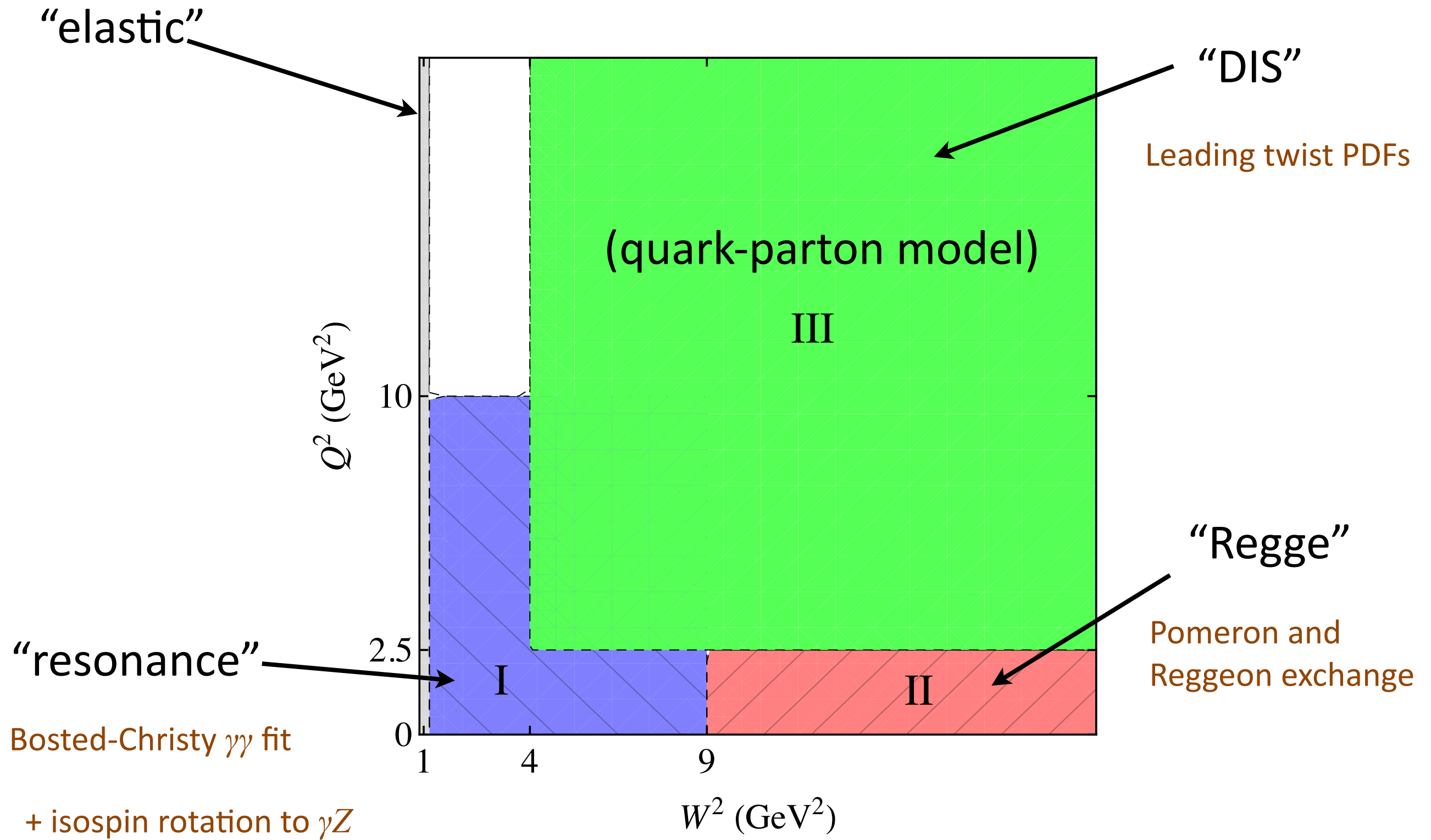
- Mainly different treatments of low  $Q^2$ , low  $W$  region background contributions
- Agree on overall magnitude of 8% correction, but disagree on errors and details

# AJM structure function model

- Accurate knowledge of  $\gamma\gamma$  and  $\gamma Z$  structure functions (at all kinematics) vital for determination of radiative corrections
  - Wealth of data on  $F_i^{\gamma\gamma}$  structure functions over large range of kinematics in  $Q^2$  and  $W$  (or  $x$ ) – with some gaps
  - Relatively little known about  $F_i^{\gamma Z}$  interference structure functions below HERA measurements, with  $Q^2 \geq 1500 \text{ GeV}^2$
  - Fit  $F_i^{\gamma\gamma}$  over all kinematics in  $Q^2$  and  $W$ , then “rotate” to  $F_i^{\gamma Z}$  using available theoretical/phenomenological constraints
- *e.g.* isospin symmetry

$$\langle N^* | J_Z^\mu | p \rangle = (1 - 4 \sin^2 \theta_W) \langle N^* | J_\gamma^\mu | p \rangle - \langle N^* | J_\gamma^\mu | n \rangle$$

# Integration region (structure function map)



# Basic issue: how to relate $F_{1,2}^{\gamma Z}$ to $F_{1,2}^{\gamma}$ ?

## Scaling region III

$$F_2^{\gamma} = \sum_q e_q^2 x(q + \bar{q})$$
$$F_2^{\gamma Z} = \sum_q 2e_q g_V^q x(q + \bar{q})$$
$$x = \frac{Q^2}{W^2 - M^2 + Q^2}$$

Resonance region I largest contribution (unlike  $F_3^{\gamma Z}$ )

For  $\gamma\gamma$  use Christy-Bosted (CB) fit to  $e-p$  cross sections

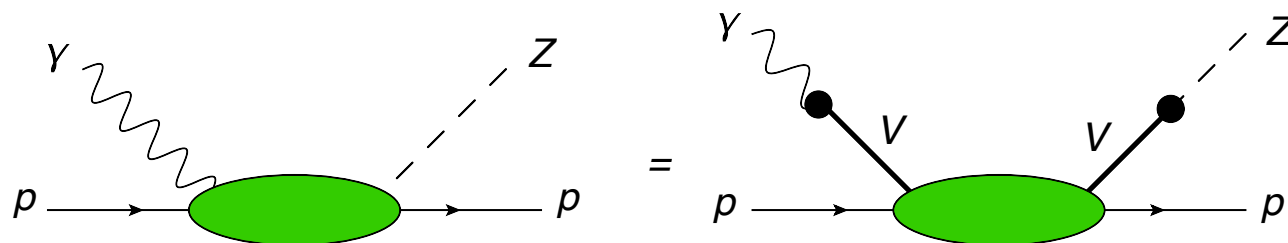
$$\sigma_{T,L} = \sigma_{T,L}(\text{res}) + \sigma_{T,L}(\text{bg})$$

- $\sigma_{T,L}(\text{res})$
- Includes 7 most prominent  $N^*$  resonances below 2 GeV.
  - Generally agrees with data to  $\sim 5\%$
  - For  $\gamma Z$  modify fit by ratio of weak to e.m. transition amplitudes.



## Background $\sigma_{T,L}(\text{bg})$

- Use Vector Meson Dominance (VMD) models fit to high energy data, plus isospin rotations



$$V = \rho, \omega, \phi + \text{continuum}$$

$$\sigma_V^{\gamma Z} = \kappa_V \sigma_V^{\gamma\gamma} \quad \frac{\sigma^{\gamma Z}}{\sigma^{\gamma\gamma}} = \frac{\kappa_\rho + \kappa_\omega R_\omega + \kappa_\phi R_\phi + \kappa_C R_C}{1 + R_\omega + R_\phi + R_C}$$

Isospin rotation:  $\kappa_\rho = 2 - 4 \sin^2 \theta_W$ ,  $\kappa_\omega = -4 \sin^2 \theta_W$ ,  $\kappa_\phi = 3 - 4 \sin^2 \theta_W$

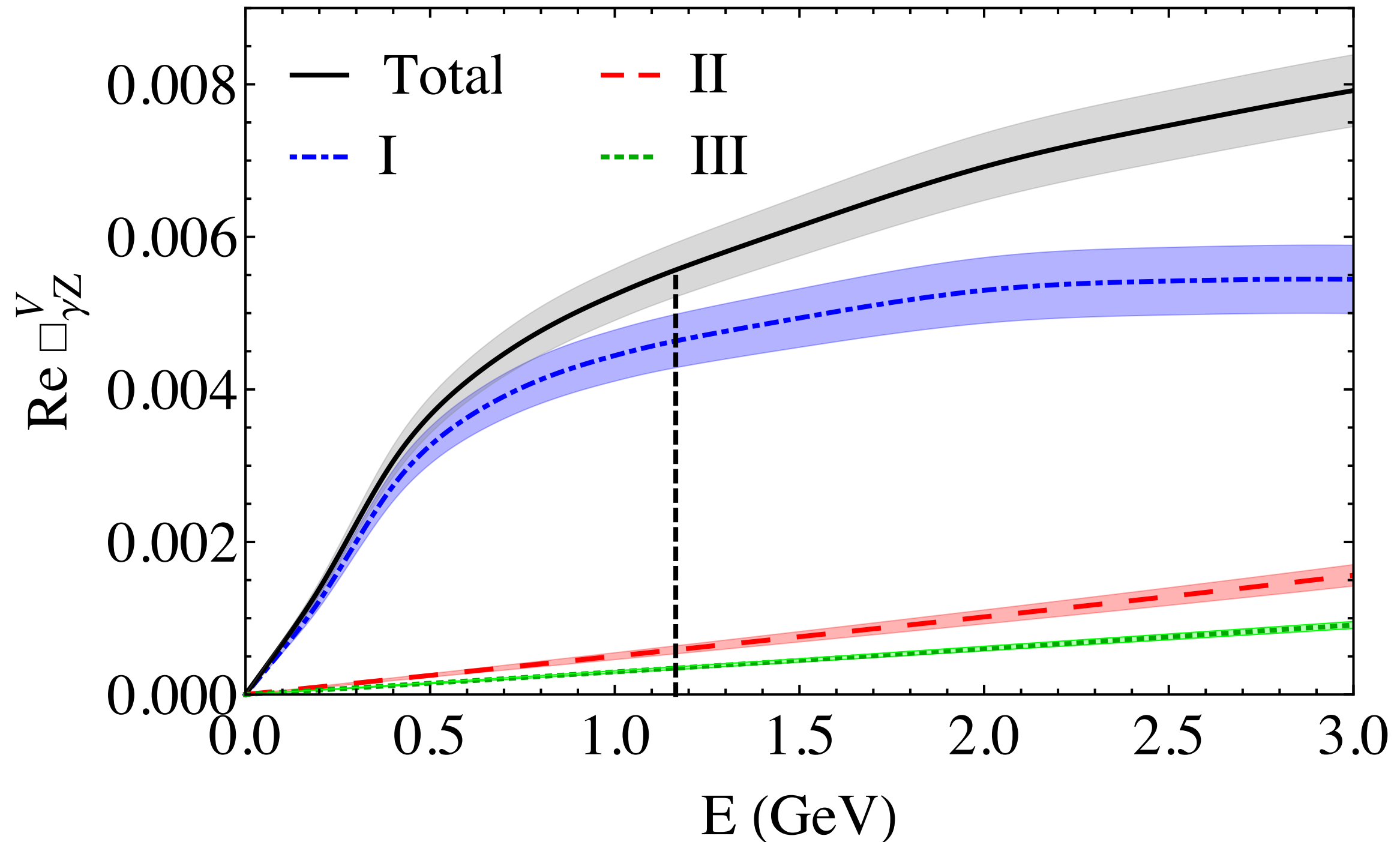
→ continuum parameter  $\kappa_C$  not constrained in VMD

- **GHRM**: assign 100% uncertainty on continuum contribution (dominates errors)

- **AJM model**: constrain continuum (higher  $Q^2$ ) contribution by matching with PDF ratios ( $\gamma Z$  to  $\gamma\gamma$ ) across boundaries of Regions I, II and III.

# Contribution from different regions to $\square_{\gamma Z}^V$

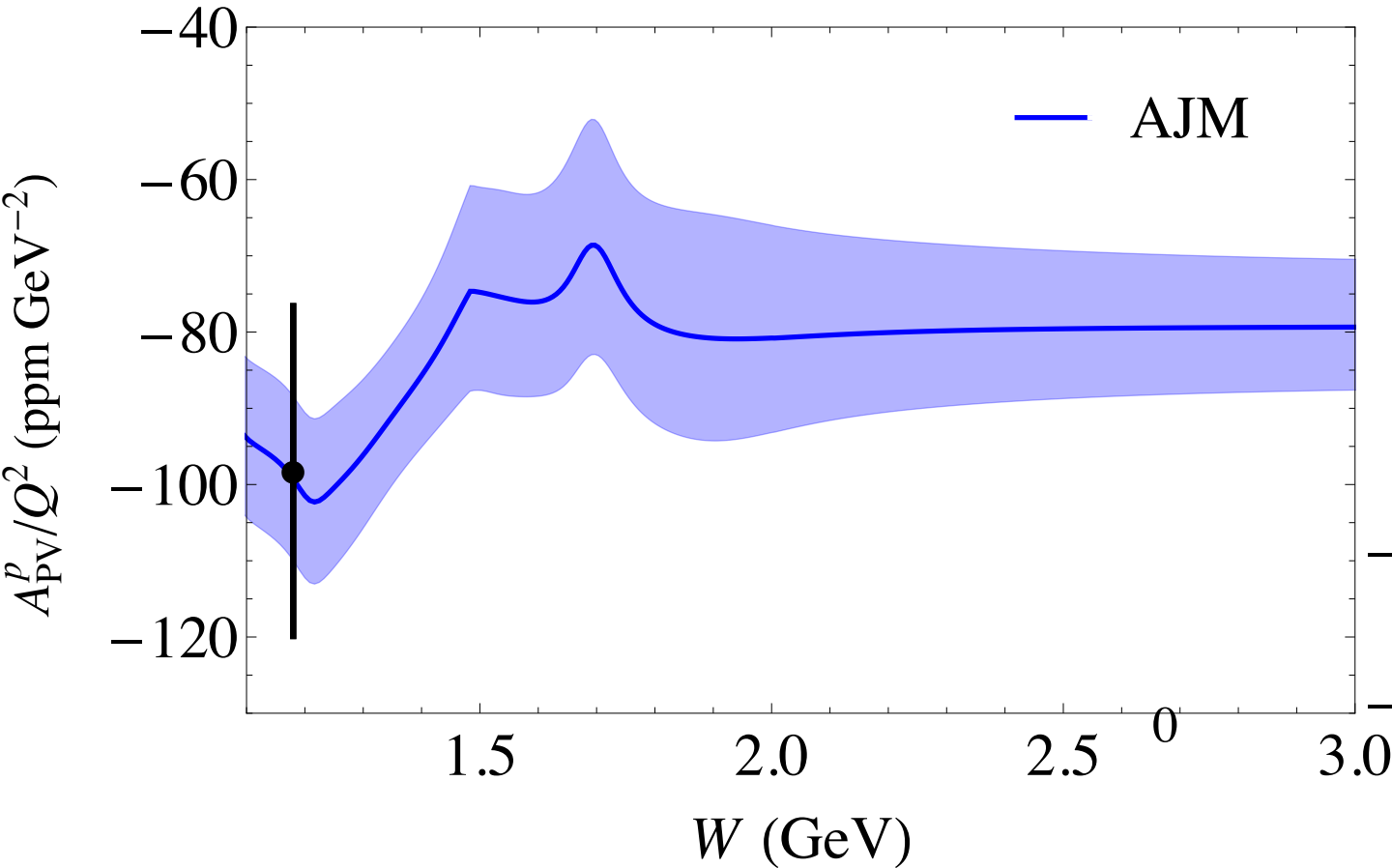
(relative to weak charge of 0.0713)



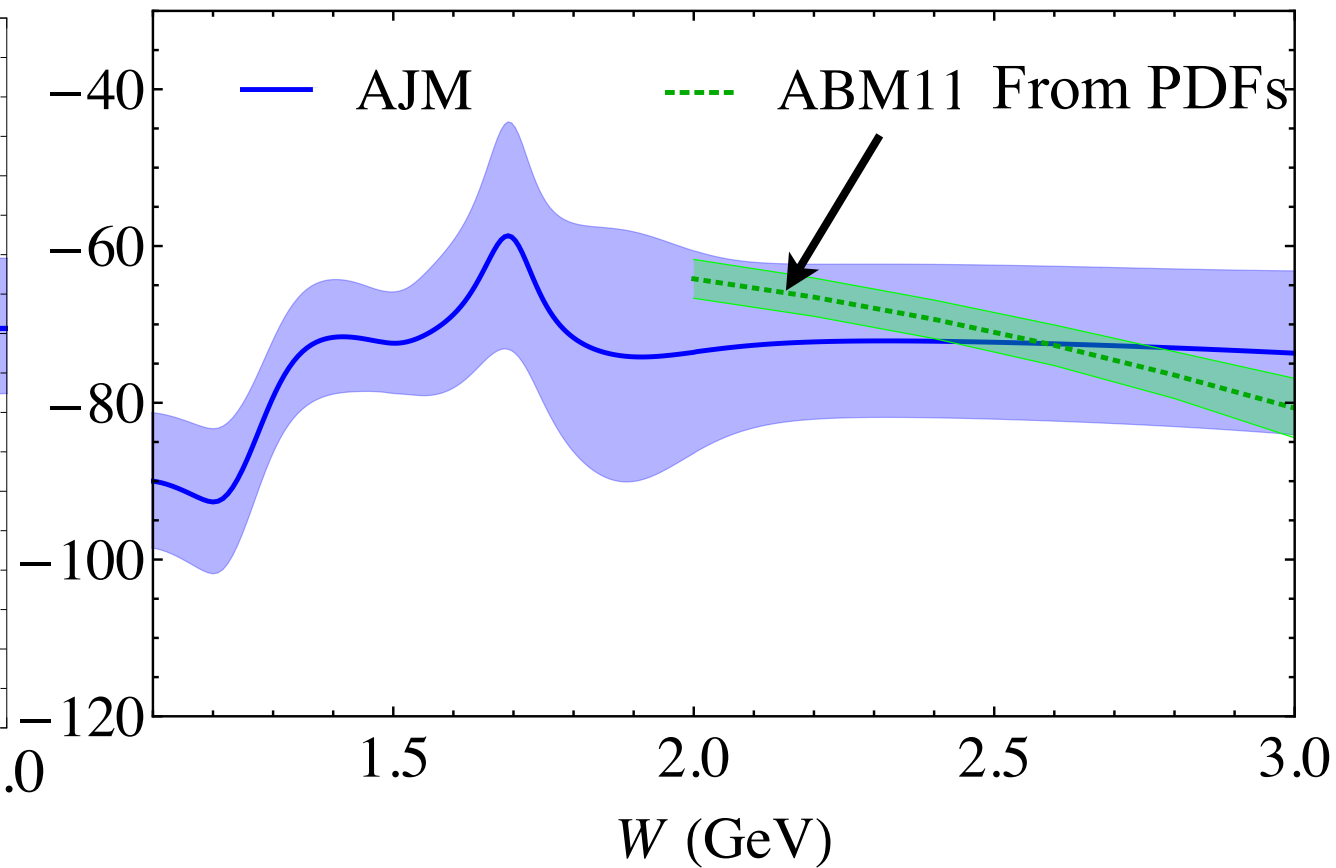
# AJM $\gamma Z$ model direct test

- Parity-violating Deep Inelastic Scattering (PVDIS) asymmetry allows a direct measurement of the  $\gamma Z$  structure functions

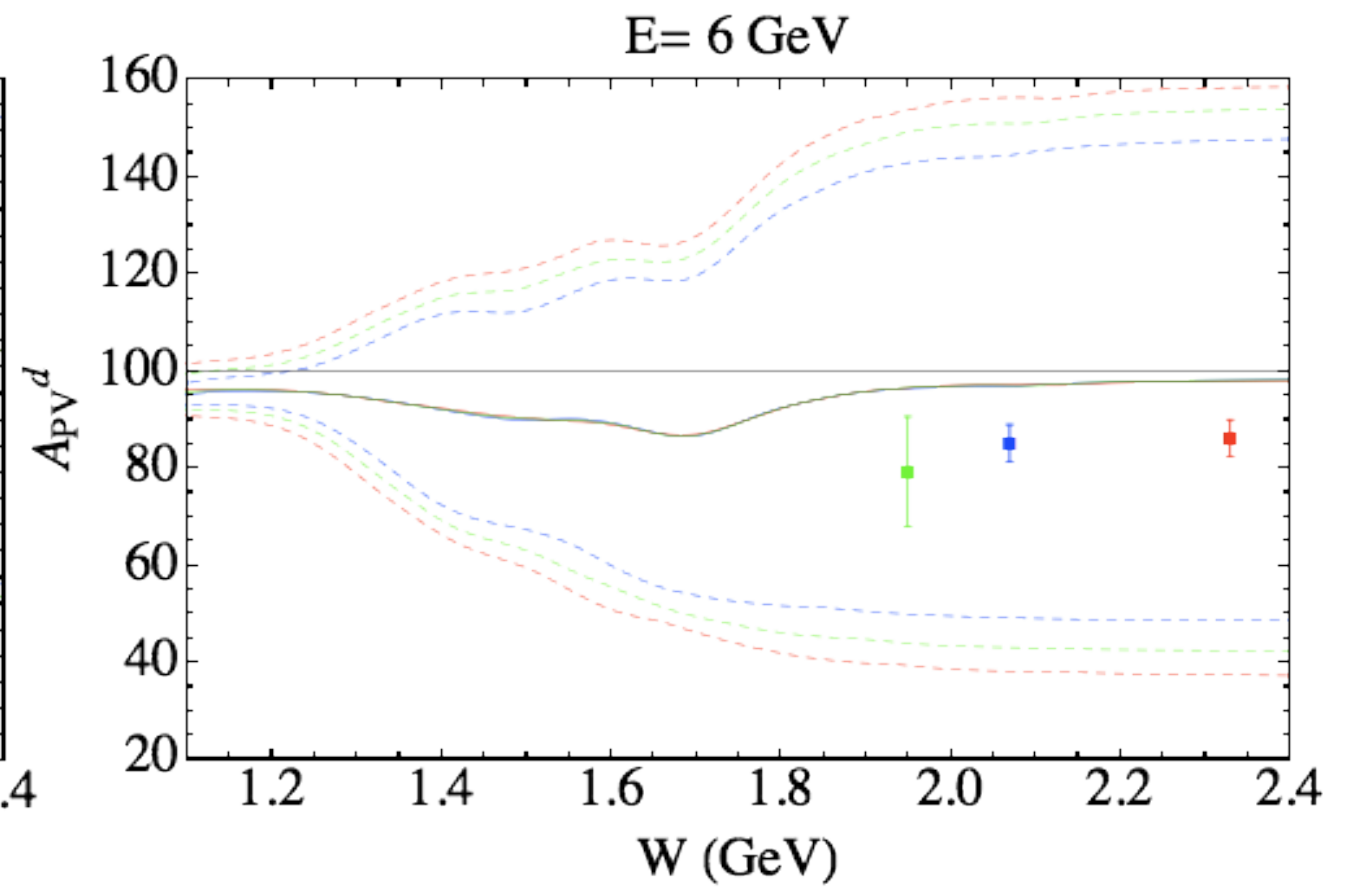
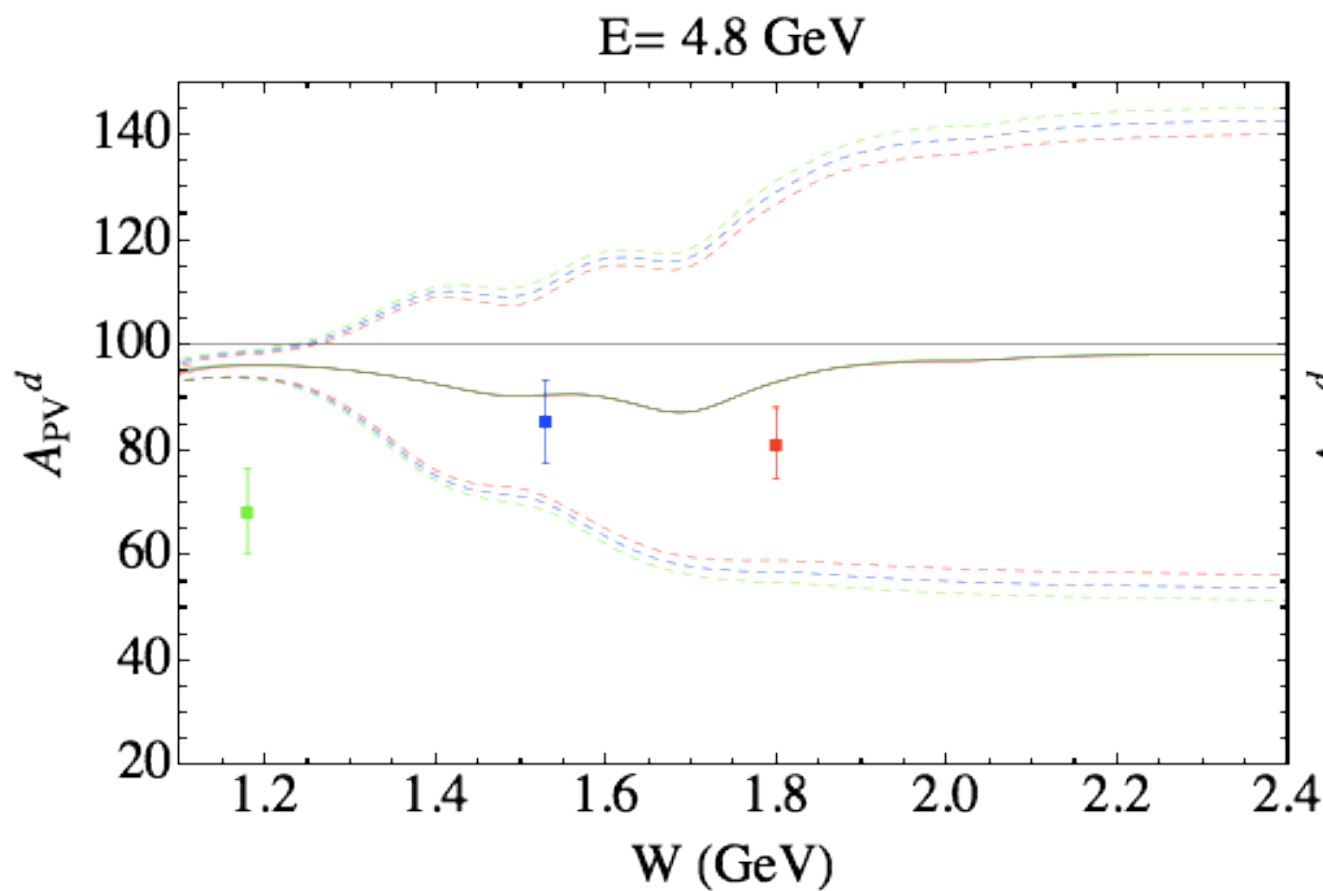
$$A_{\text{PV}} = g_A^e \left( \frac{G_F Q^2}{2\sqrt{2}\pi\alpha} \right) \frac{xy^2 F_1^{\gamma Z} + (1-y)F_2^{\gamma Z} + \frac{g_V^e}{g_A^e} (y - y^2/2)x F_3^{\gamma Z}}{xy^2 F_1^{\gamma\gamma} + (1-y)F_2^{\gamma\gamma}}$$



$Q^2=0.34 \text{ GeV}^2, E=0.69 \text{ GeV}$

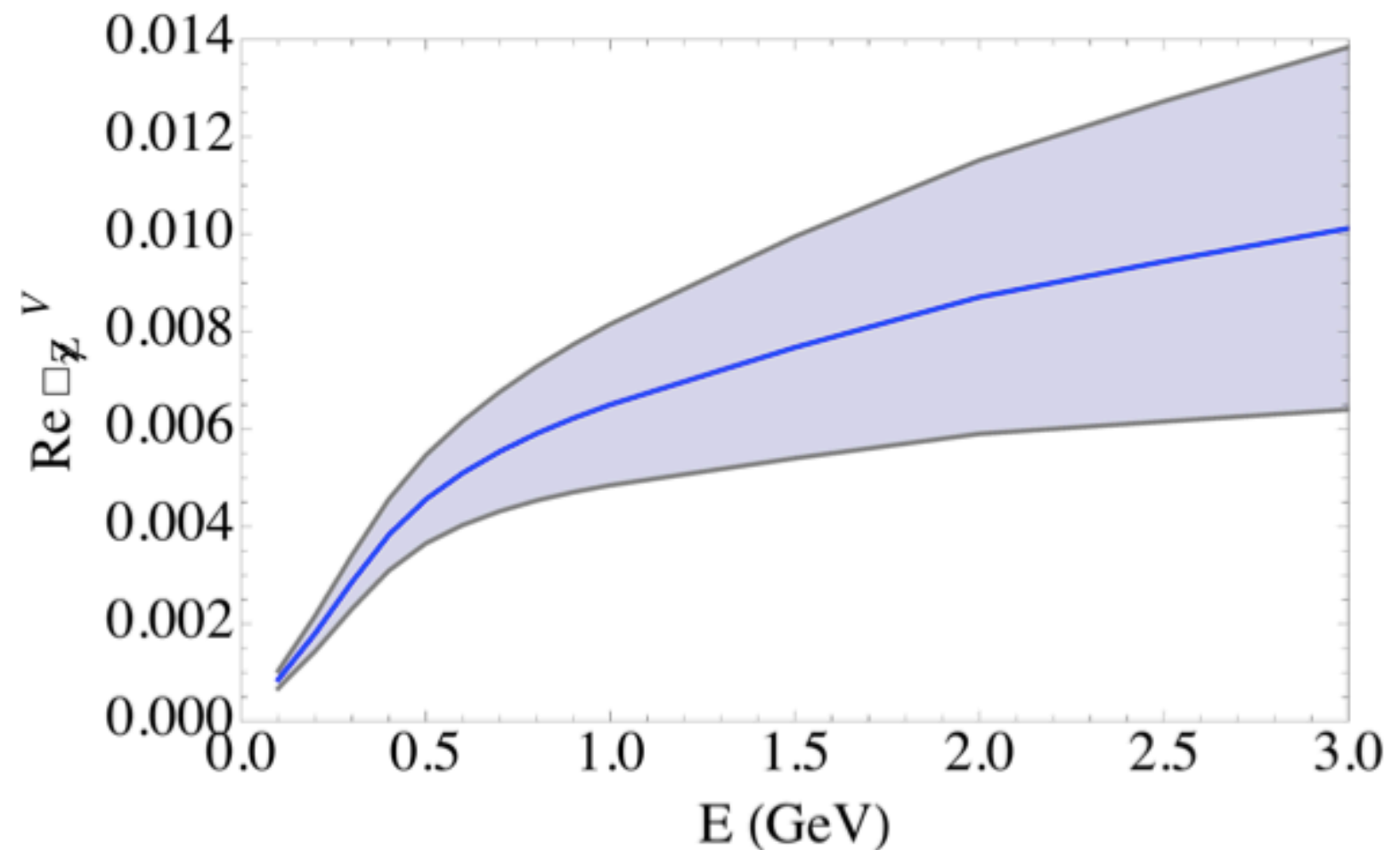


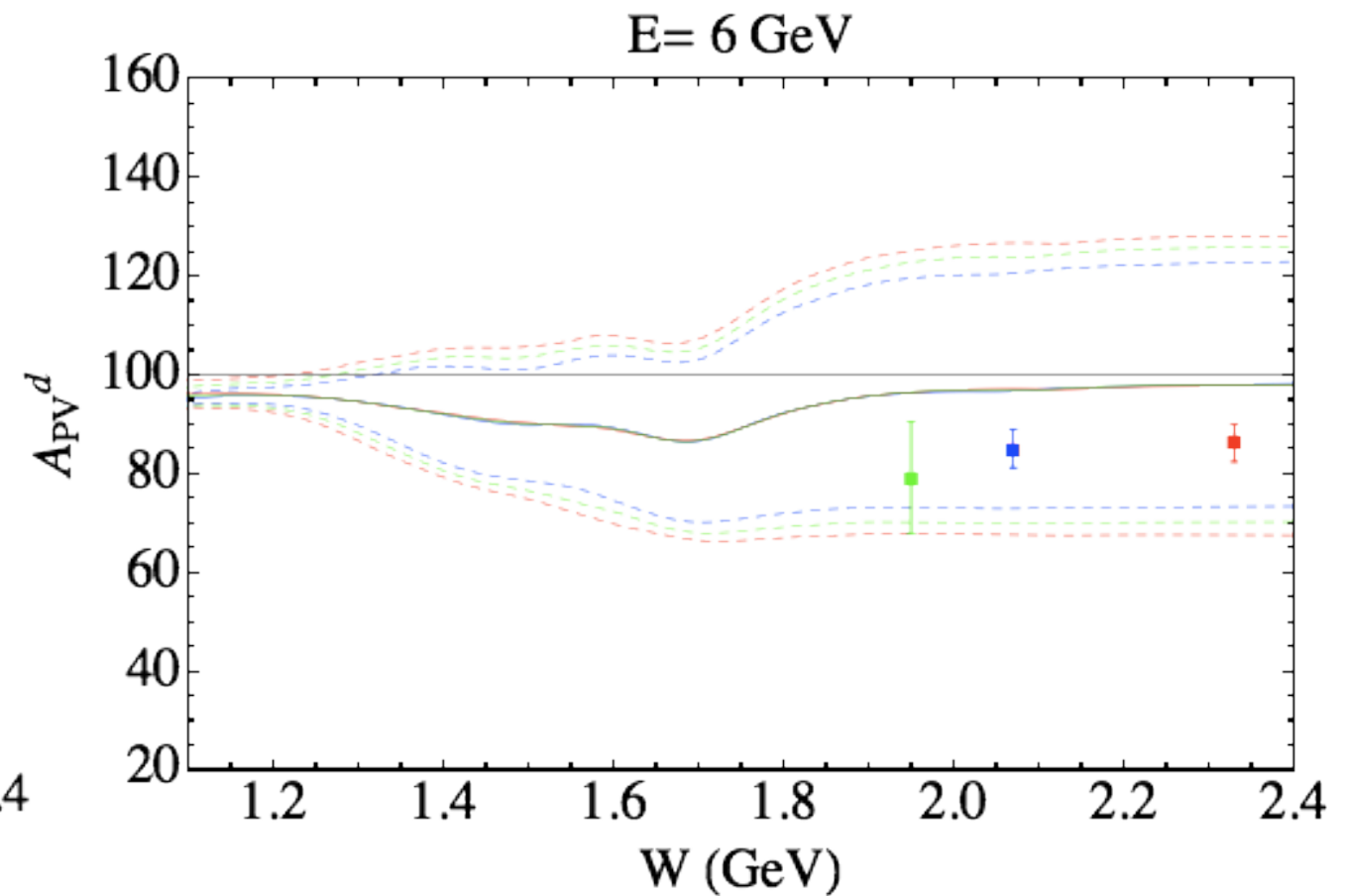
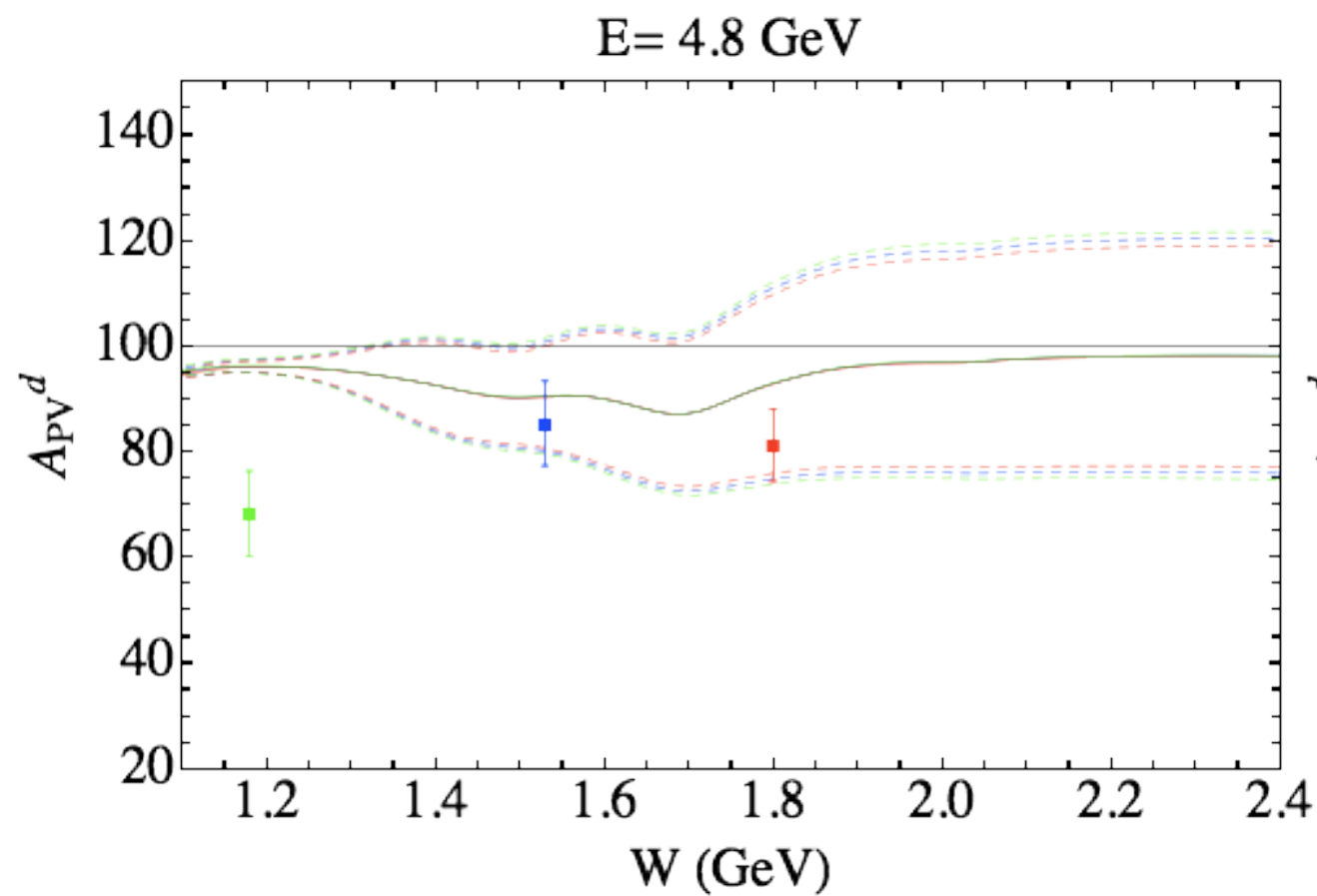
$Q^2 = 2.5 \text{ GeV}^2, E = 6 \text{ GeV}$



Potential impact of  
constraints from  
deuteron PV inelastic  
asymmetries

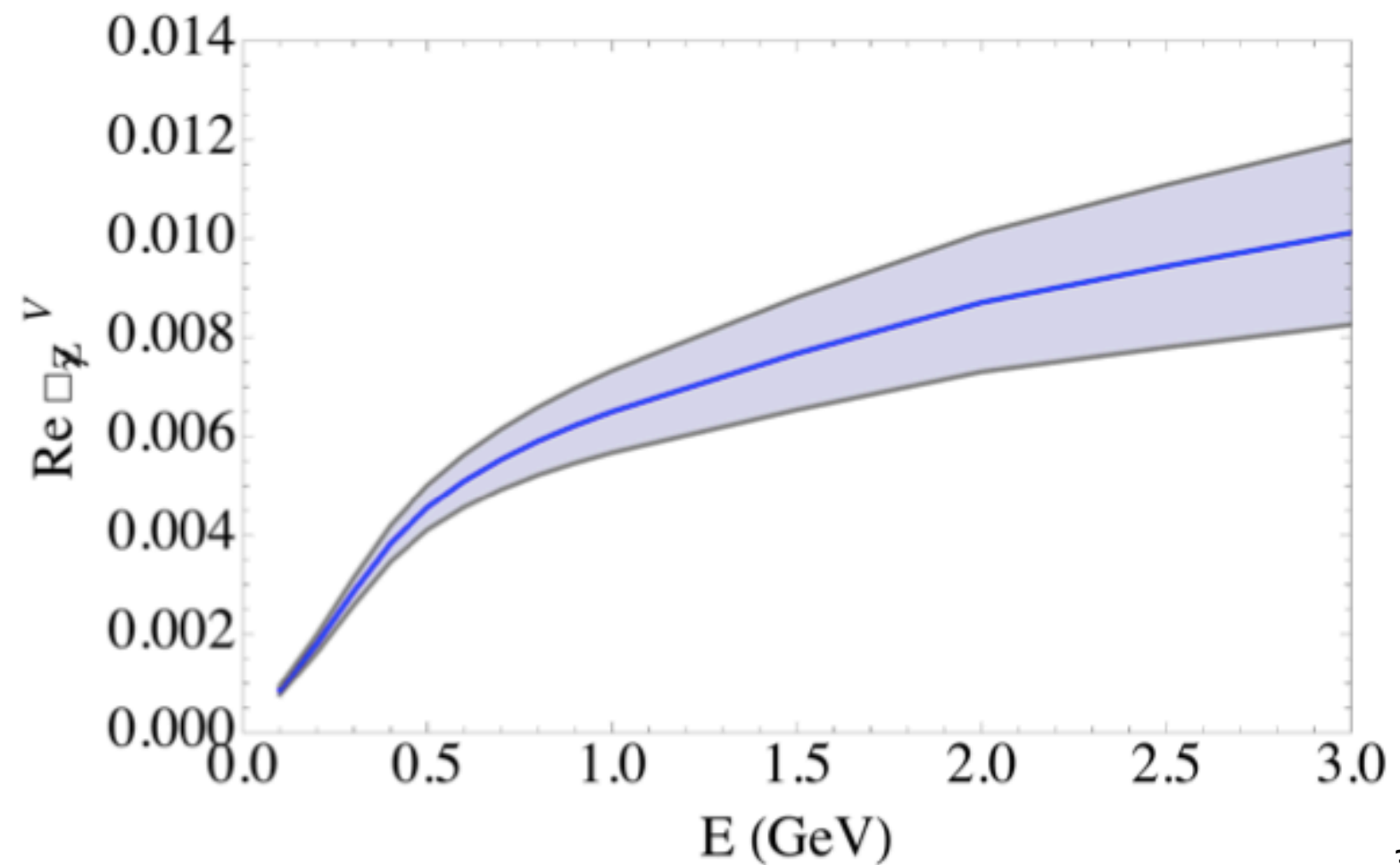
100% uncertainty on  
continuum background

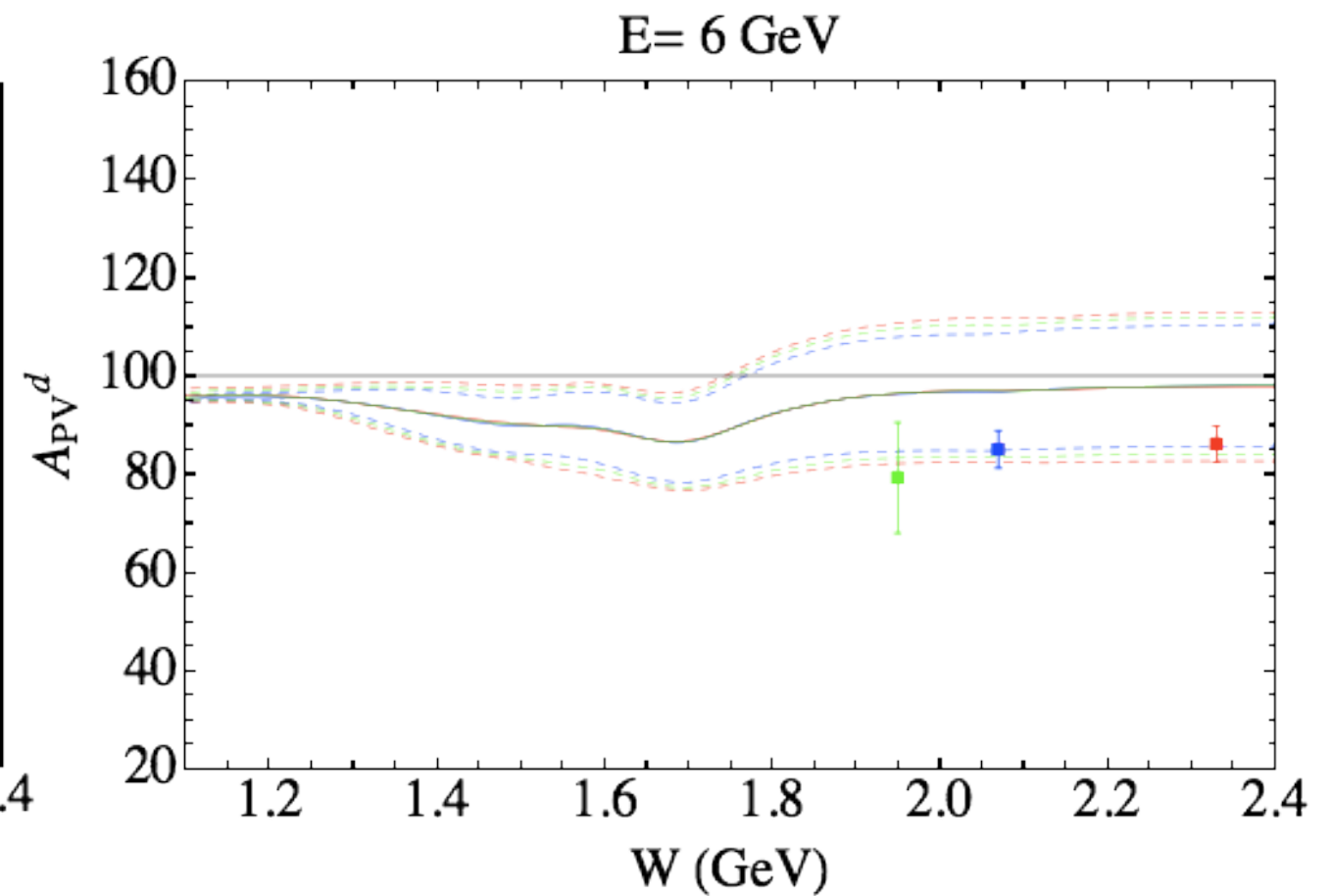
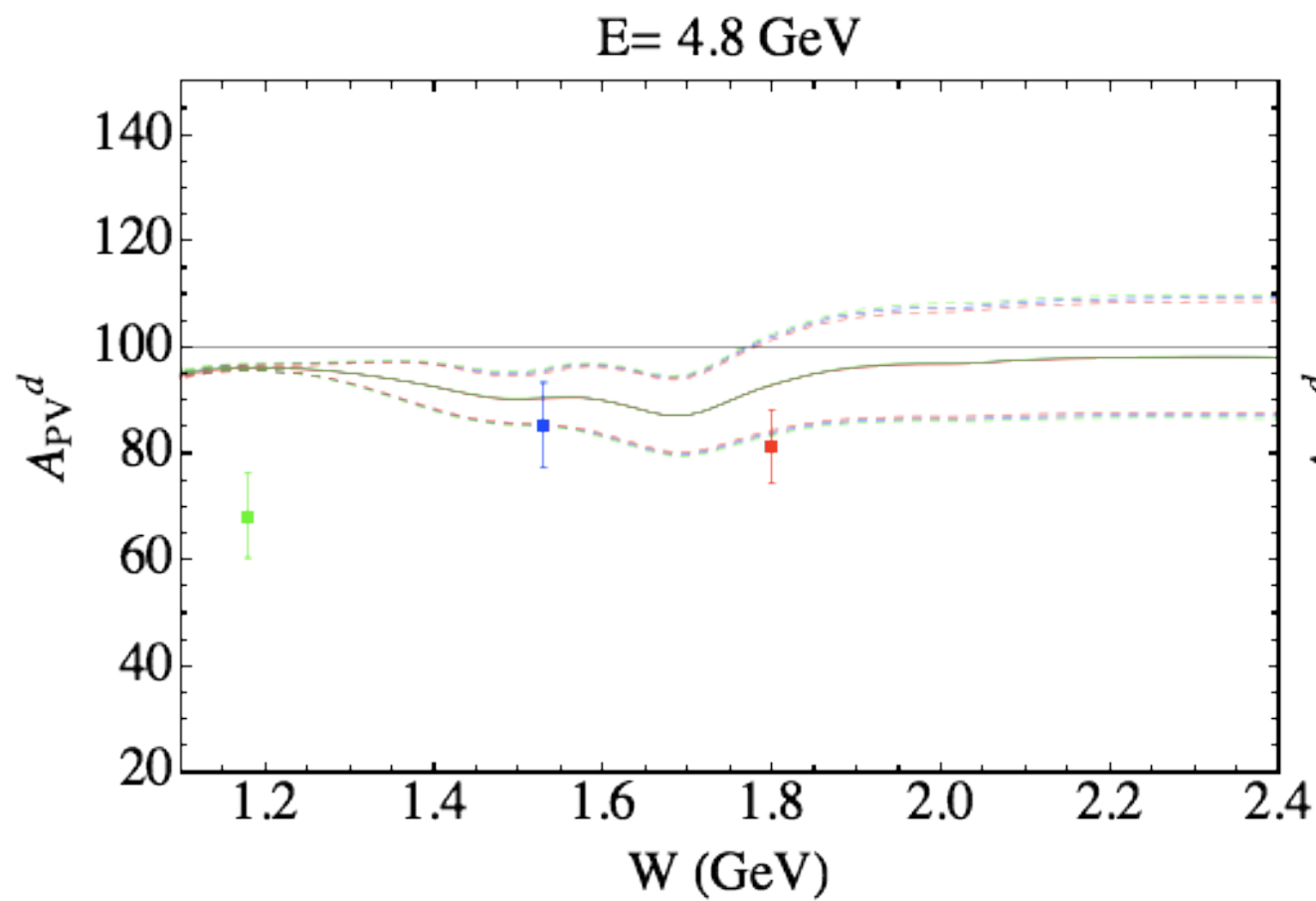




Potential impact of  
constraints from  
deuteron PV inelastic  
asymmetries

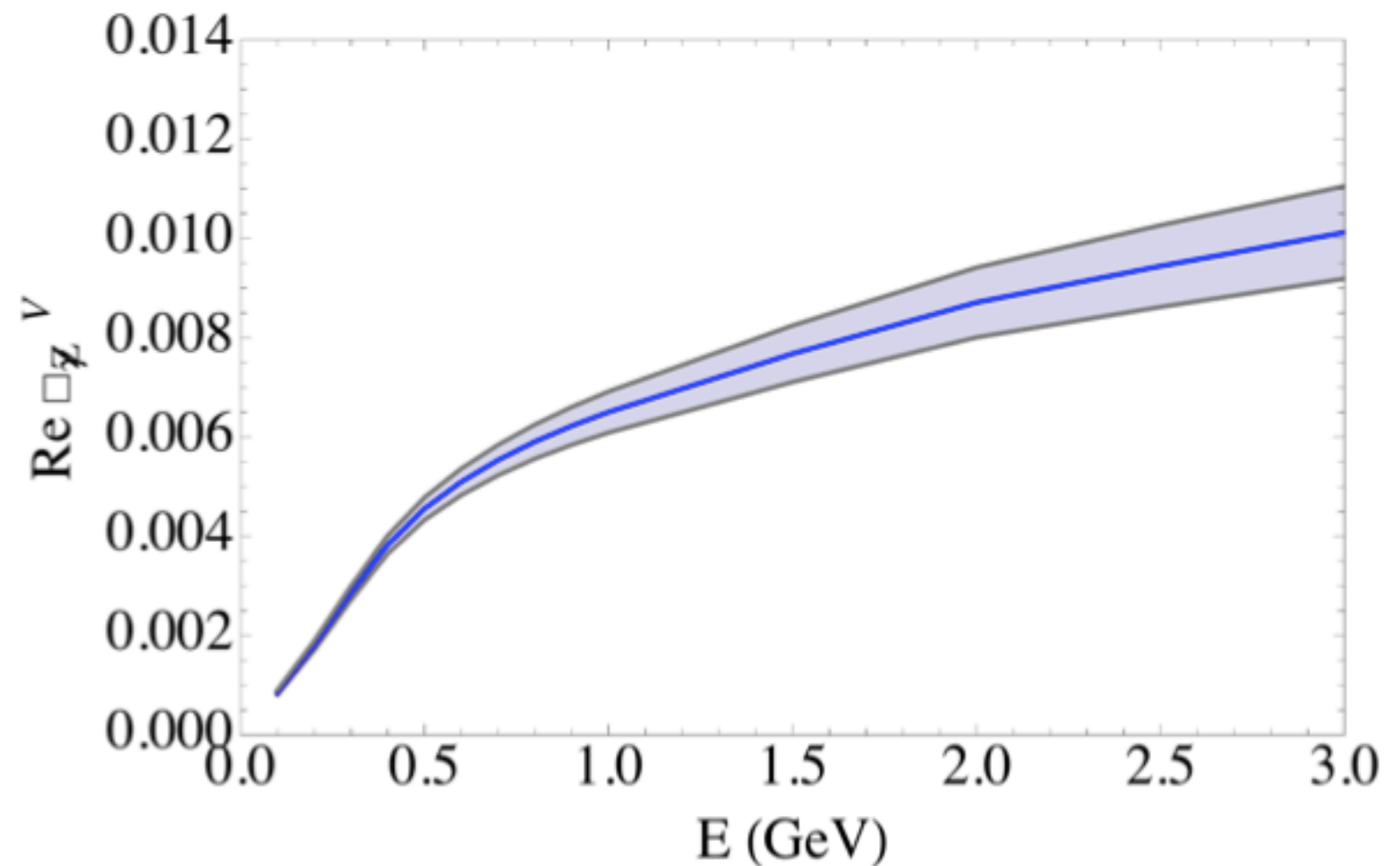
50% uncertainty on  
continuum background



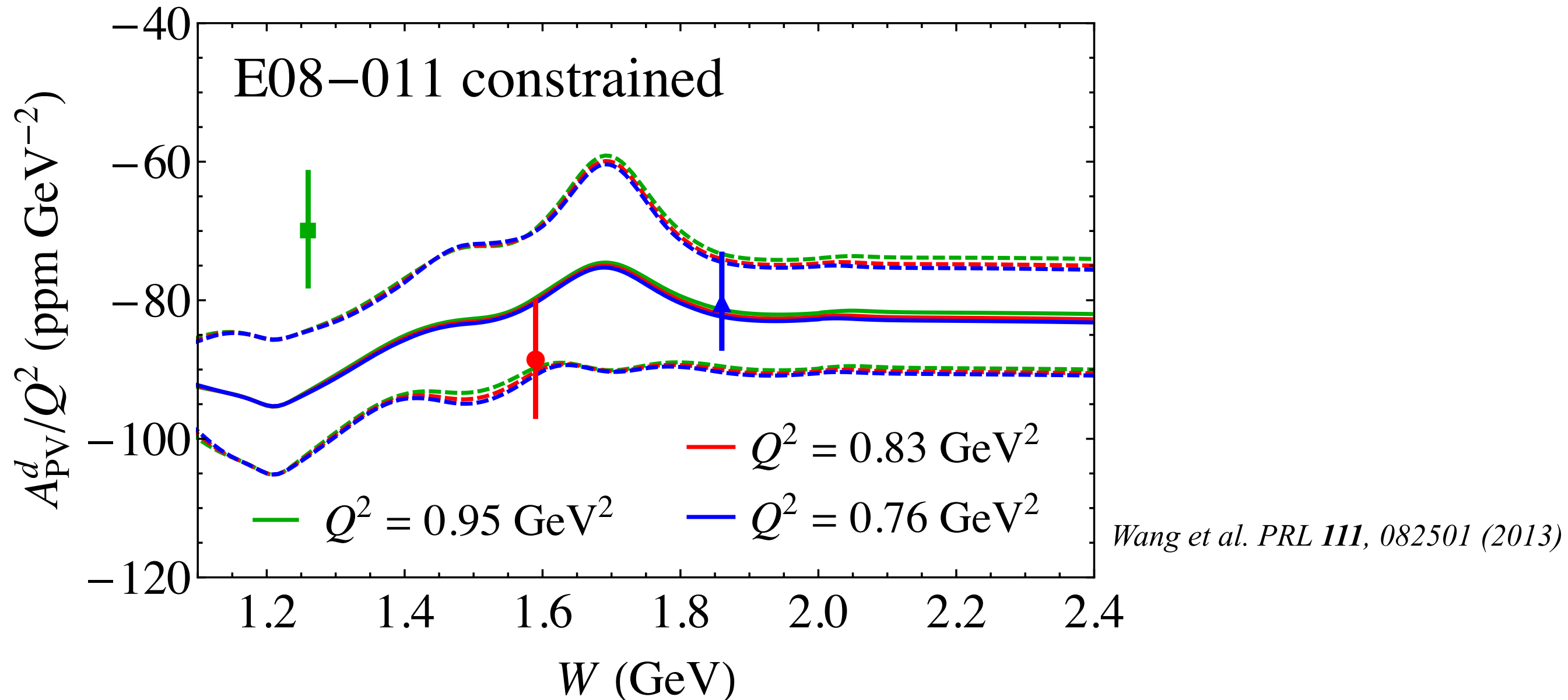


Potential impact of  
constraints from  
deuteron PV inelastic  
asymmetries

25% uncertainty on  
continuum background



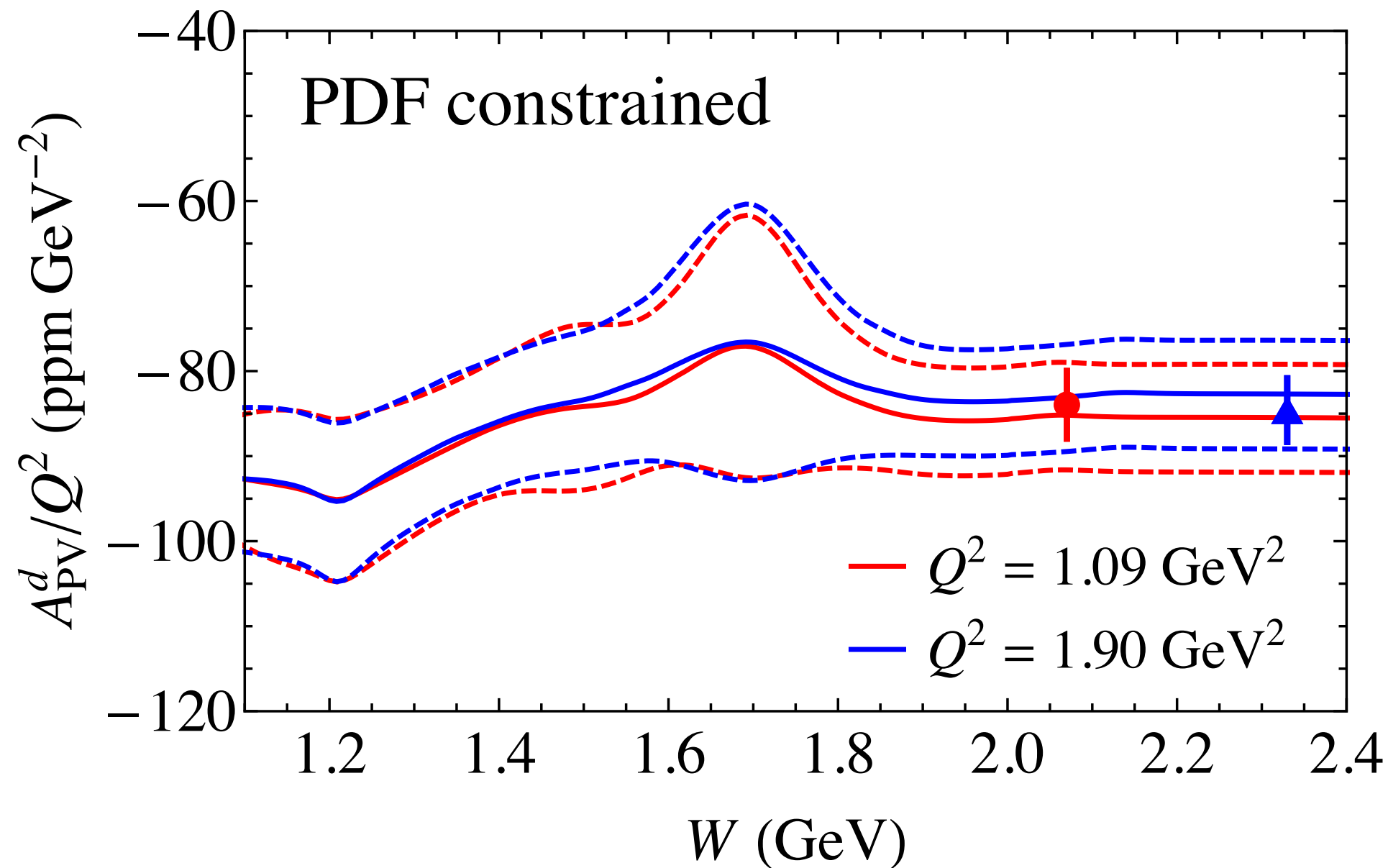
# Constraints from PV inelastic asymmetries



AJM model asymmetries and uncertainties for PV  
deuteron asymmetry constrained by fit to E08-011 data

*Hall et al. (2013)*

# Predictions for PV deuteron asymmetry in DIS kinematics



**Prediction:** *Hall et al. (2013)*

$$A_{PV} = -92.4 \pm 6.8 \text{ ppm}$$

$$A_{PV} = -157.2 \pm 12.2 \text{ ppm}$$

**E08-011:** *Wang et al. Nature 506, 67 (2014)*

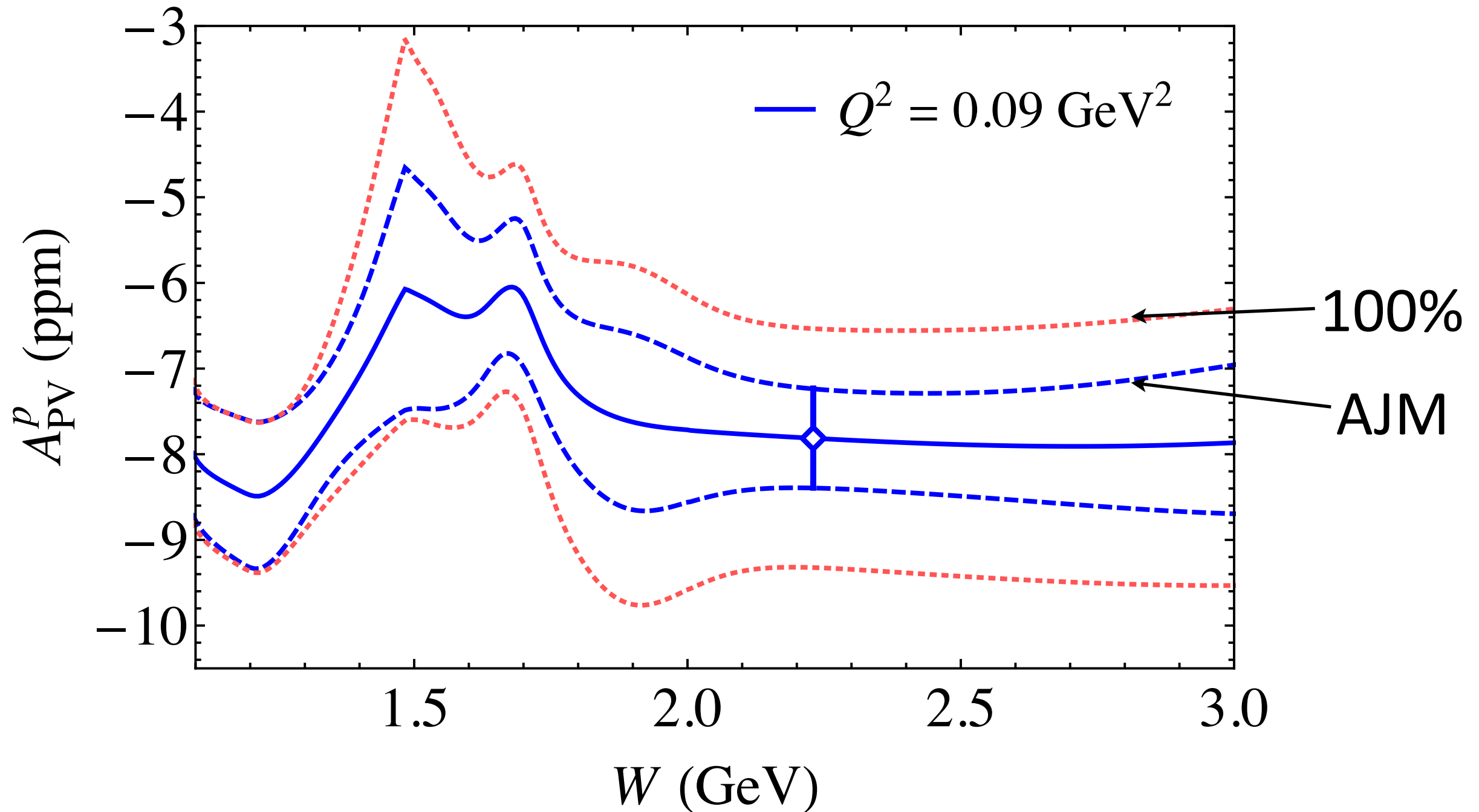
$$A_{PV} = -91.1 \pm 4.3 \text{ ppm}$$

$$A_{PV} = -160.8 \pm 7.1 \text{ ppm}$$



# Parity-violating inelastic asymmetries

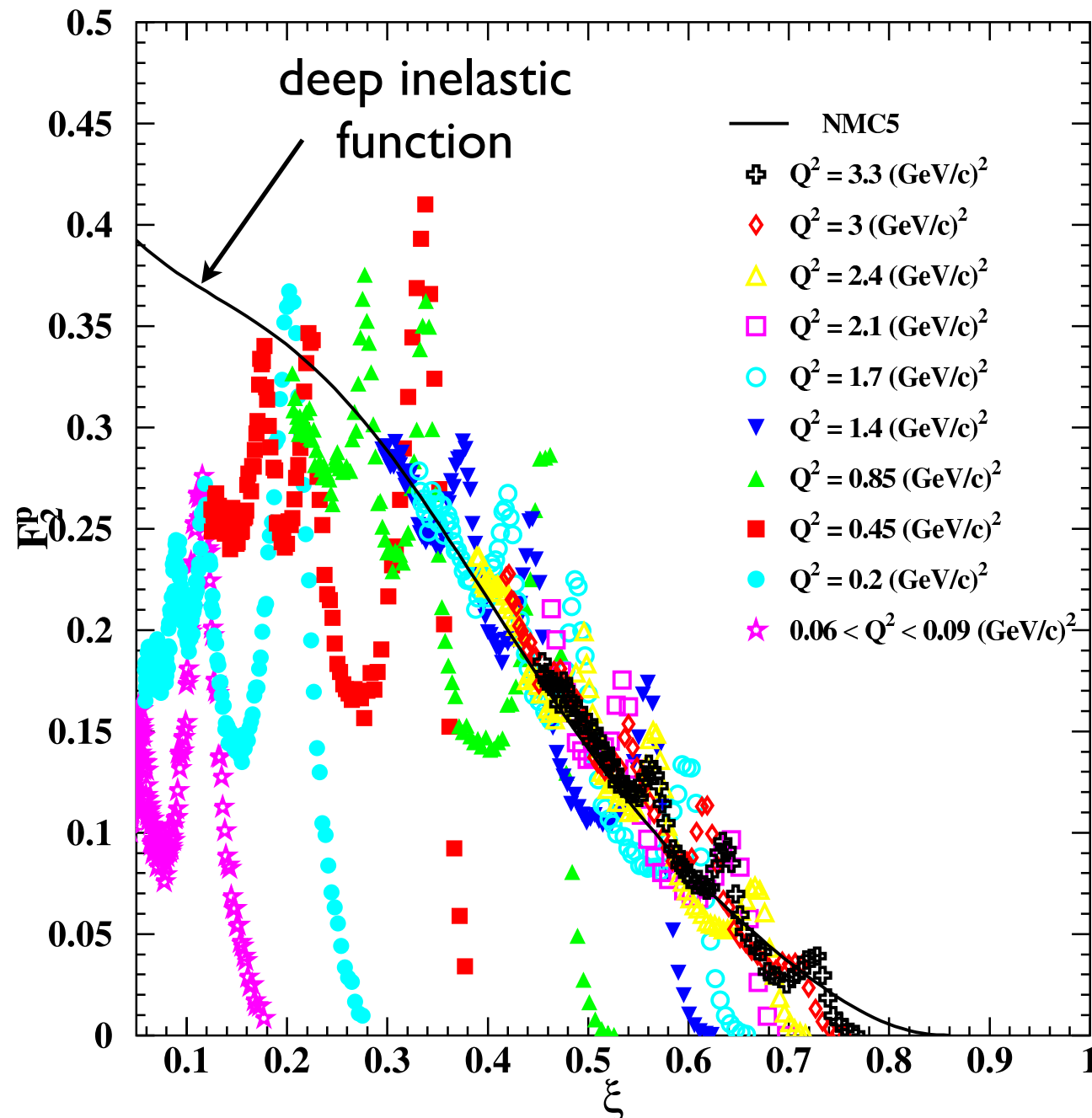
- Expected inelastic asymmetry data from Qweak



→ AJM model uncertainties compared with 100% on continuum contribution

*Hall et al. (2013)*

# Duality in electron-nucleon scattering



*Niculescu et al., PRL 85, 1182 (2000)*  
*WM, Ent, Keppel, PRep. 406, 127 (2005)*

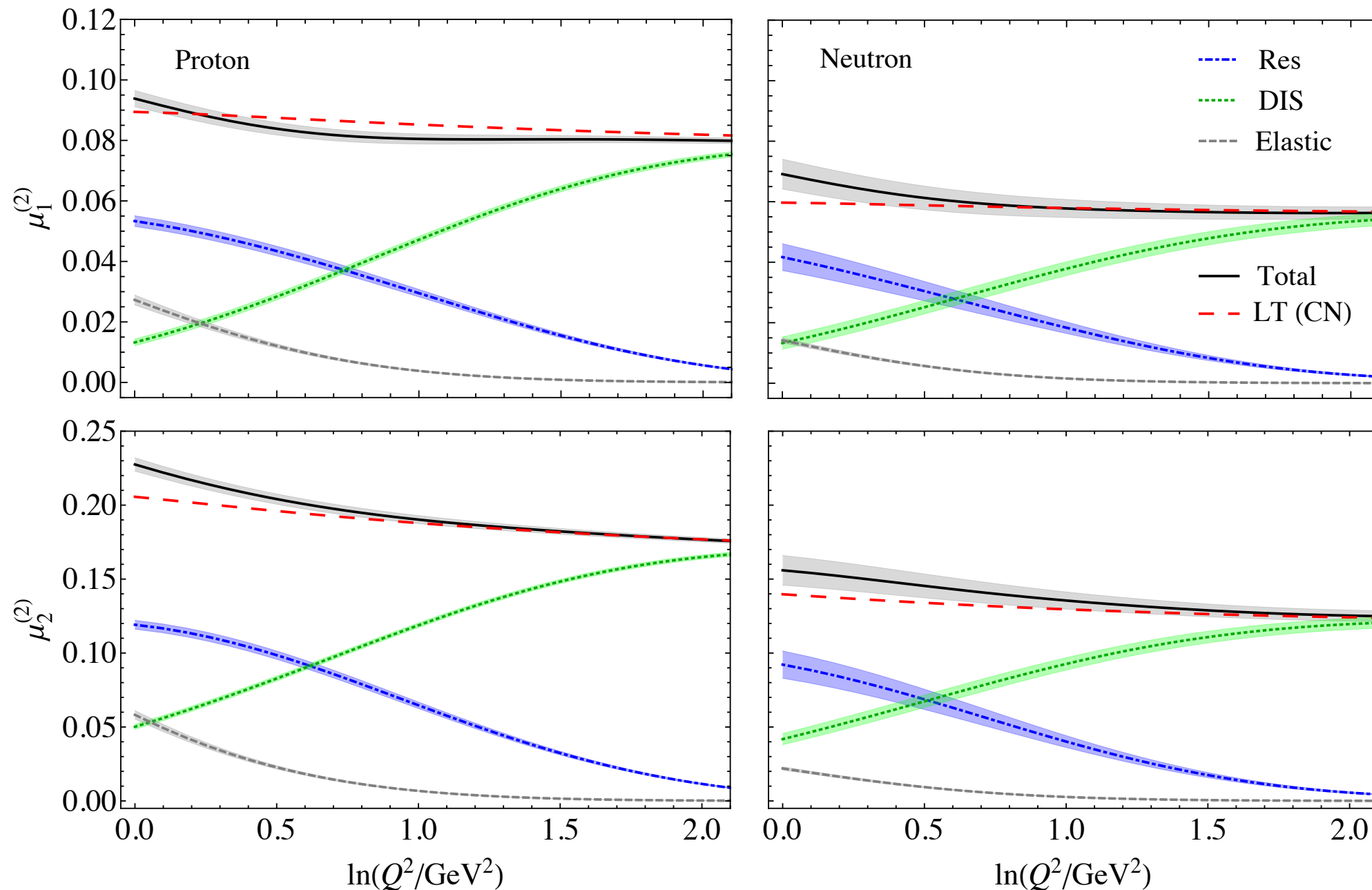
average over  
 (strongly  $Q^2$  dependent)  
 resonances  
 $\approx Q^2$  independent  
 scaling function

“Nachtmann” scaling variable

$$\xi = \frac{2x}{1 + \sqrt{1 + 4M^2 x^2 / Q^2}}$$

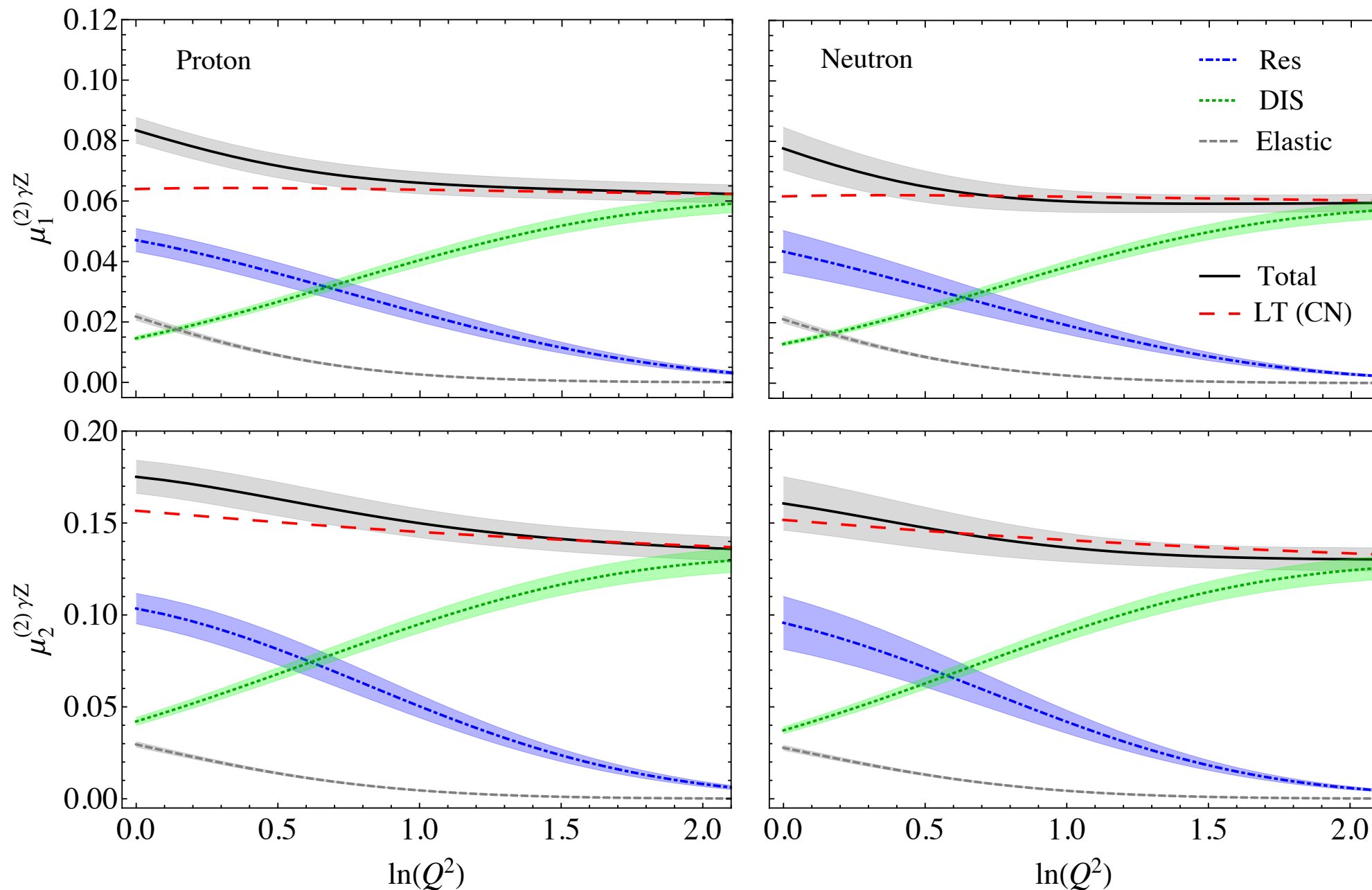
Separates higher twist (HT) effects  
 from target mass corrections to  
 leading twist (LT)

# $\gamma\gamma$ Leading Twist (LT) $F_{1,2}$ moments vs. Nachtmann moments



- Compare total empirical moments of structure functions to leading twist (LT) contributions down to low  $Q^2$
- Difference indicative of higher twist (HT) contributions
- Sum is approximately independent of  $Q^2$
- Note isospin independence  $\longrightarrow$  Apply to  $\gamma Z$  structure functions?

# $\gamma Z$ Leading Twist (LT) moments vs. Nachmann



Allows us to extend PDF region down to  $Q^2=1$  GeV<sup>2</sup> (from  $Q^2=2.5$ )

$$\square_{\gamma Z}^V @ 1.165 \text{ GeV} : \quad (5.6 \pm 0.4) \times 10^{-3}, \quad 2013$$

$$(5.4 \pm 0.4) \times 10^{-3}, \quad 2015$$

# Summary

- Lots of interesting new theoretical work motivated by new experimental results
- Dispersive method only feasible approach for TPE, with connection to data in forward angle limit
- Efforts underway to incorporate electroproduction data throughout the resonance region, including background
- Clear need for definitive  $e^+p$  measurements at high  $Q^2$ , low  $\varepsilon$
- Dispersion approach significant improvement over old methods
- PDF region provides constraints on model-dependence of isospin rotation
- Direct comparison with PV inelastic data in resonance and DIS regions
- e-d PVDIS asymmetry strongly constrains the uncertainty
- checking  $\Delta$  region at Mainz or JLab would be useful
- quark-hadron duality approach allows further constraints on uncertainties